Intracellular Trafficking Regulators for the Atherogenic Lipoproteins LDL and Lp(a)

by

Taslima Gani Khan

A dissertation submitted in partial fulfillment
of the requirements for the degree of
Doctor of Philosophy
(Chemical Biology)
in the University of Michigan
2022

Doctoral Committee:

Assistant Professor Brian T. Emmer, Co-Chair
Professor David Ginsburg, Co-Chair
Assistant Professor Ryan Baldridge
Associate Professor Tomasz Cierpicki
Professor Ryoma Ohi

Taslima G. Khan

khantg@umich.edu

ORCID iD: 0000-0002-4778-6659

Acknowledgements

I would like to express my gratitude to all those people, whose incredible support has made it possible for me to navigate through the journey of my PhD. First and foremost, I am extremely grateful to my advisors, Dr. David Ginsburg and Dr. Brian Emmer for their continuous guidance throughout my PhD and for always being supportive of my career goals. I will forever be indebted to David for providing such a positive work environment to grow as a scientist and giving me the freedom to explore my scientific interests, for always being patient and for all his invaluable advice about career and life. I will always be thankful to Brian for his invaluable supervision, encouragement, and persistent optimism, for believing in my abilities more than I did and always helping me build my confidence. I would also like to thank the rest of my thesis committee: Dr. Ryan Baldridge, Dr. Ryoma Ohi, and Dr. Tomasz Cierpicki for their insightful suggestions, and career advice. I will always appreciate the support provided by my former supervisor, Dr. Kristin Koutmou for encouraging me to apply to the PhD program. I am so glad that I was able to pursue my PhD at the University of Michigan where I learned so much and met so many incredible people. I would also like to acknowledge with much appreciation the crucial role of our lab manager, David Siemieniak, administrative assistant, Suzann Labun and research staffs Beth and Guojing in managing everything in the lab that helps smooth running of our research and for their active help and co-operation whenever needed. My sincere gratitude also goes to my lab mates for their support, scientific insights, and stimulating discussions. Thank you, David and Audrey, for teaching me the basics of RT-qPCR. Thank you, Candi, Matt and Laura, for always helping me with preparing presentations. Thank you Prabhodh and Laura for

being my go-to people for troubleshooting experiments and for always being such supportive colleagues. Thank you Vi for your all your input and suggestions. Thank you, Candi, for being my coffee mate and critical thinking companion and for always being there when I needed emotional support. I am so glad you joined the Ginsburg lab. I will always cherish our friendship and time spent together. I would also like to appreciate all my friends (Ayesha, Rumana, Shameera & Preethi) for their encouragement and support. Special thanks to Shameera, for taking care of my daughter for one entire school year during the pandemic, when classes were virtual. Also, thanks to Preethi for looking after my daughter countless numbers of days while I worked in the lab. I could not have completed my projects without your selfless help.

Finally, I would like to thank my family for encouraging me to chase my dreams. I could never have achieved anything in life without the unconditional love and support of my parents, brother & sister through every stage of my life. Thanks for being patient and understanding me for not visiting home for the last 4 years. Thanks also to my husband for his tremendous understanding, encouragement & moral support while we were physically distant for three and a half years as I continued my PhD. And most importantly, thanks to my daughter Sanayah for being the pillar of support & putting up with me being in the lab or studying at home and ignoring her requests to spend time with her countless numbers of times. Thanks for never complaining every time I took you to the lab and for patiently waiting while I completed my work. Thanks for being so mature for your age & for understanding that this was for our better future.

Table of Contents

List of Figures

Abstract

Elevated levels of low-density lipoprotein (LDL) and its derivative lipoprotein(a) (Lp(a)) in the bloodstream are directly implicated in the development and progression of atherosclerotic cardiovascular diseases (ASCVD). LDL homeostasis is mainly regulated by the LDL receptor (LDLR), which is expressed predominantly on the cell surface of hepatocytes where it binds and removes free LDL particles from circulation. Endocytosed LDLR may then either be recycled back to the cell surface or diverted to lysosomes for its degradation. LDLR recycling is therefore critical for efficient LDL uptake. Endocytic recycling is a complex process involving several trafficking steps and many potential molecular mediators. Here I characterized the role of a small GTPase, RAB10, in the trafficking of LDLR. I found that RAB10 depletion inhibits LDLR recycling from endocytic recycling compartment (ERC), thereby reducing surface LDLR abundance and cellular LDL uptake. Further investigation showed that RAB10 also promotes recycling of another cell surface receptor, the transferrin receptor (TFR), but from a different endocytic compartment. Our findings suggest that RAB10 impacts recycling of LDLR and TFR by promoting vesicle trafficking from different intracellular compartments.

Although Lp(a) is another casual risk factor for ASCVD, there are no specific Lp(a)-lowering treatments, and their development is limited by a gap in knowledge regarding Lp(a) regulation. Unlike the well-known receptor mediated pathway for LDL homeostasis, the mechanism(s) for cellular uptake of Lp(a) are poorly understood, and several receptors, including LDLR, have been individually studied with conflicting data. To address this gap, we applied a high-throughput whole-genome CRISPR screen to interrogate the regulators of Lp(a)

endocytosis in HuH7 cells. Surprisingly, LDLR and other known regulators of LDLR, including SCAP, MBTPS2, MYLIP were among the top hits in the screen. No other receptors, including those previously proposed to serve as Lp(a) receptors, exhibited a functional influence on Lp(a) uptake in this screen. Our results suggest that the LDL receptor is the primary mediator of Lp(a) uptake in hepatocytes. Collectively, the work done in this thesis increases our understanding of receptor mediated trafficking of LDL and Lp(a).

Chapter 1 Introduction

Cholesterol is an important biomolecule required by the human body to play several essential functions. It is a crucial structural component of cell membranes and serves as a precursor for the synthesis of vitamin D, bile acid, and steroid hormones. Cholesterol also plays a role in many signaling pathways. The majority of cholesterol required by our body is synthesized by the liver, with the remainder derived from dietary absorption in the intestine. Cholesterol is a hydrophobic lipid and therefore requires packaging within specialized lipid-protein particles called lipoproteins for transport through the bloodstream. Plasma lipoproteins are classified into five major groups based on their size and density, which is determined by their protein to lipid ratio. These includes: -1. Chylomicrons, 2. Very low-density lipoproteins (VLDL), 3. Intermediate density lipoproteins (IDL), 4. Low-density lipoproteins (LDL), and 5. High-density lipoproteins (HDL).

Although important for several physiological functions, dysregulated cholesterol homeostasis can lead to hypercholesterolemia, a leading risk and causal factor for atherosclerotic cardiovascular diseases (ASCVD)[2-4]. Atherosclerosis is a complex pathological process, in which plaque composed of cholesterol, calcium, fat, and other substances accumulates in arterial walls. Progression of atherosclerosis is associated with hardening and narrowing of arteries leading to an obstruction of blood flow. An atherosclerotic plaque can also acutely rupture and serve as a nidus for acute thrombus formation, leading to devastating consequences such as

myocardial infarction and stroke. The two well-established atherogenic lipoproteins associated with development and progression of atherosclerosis are LDL (Low density lipoprotein) and Lp(a) (Lipoprotein(a)), a derivative of LDL. Despite advances in diagnosis, treatment and prevention, atherosclerotic cardiovascular diseases remain the leading cause of death worldwide. In this chapter, we will discuss the currently understood mechanisms for LDL and Lp(a) regulation.

1.1 Regulation of plasma LDL by receptor mediated endocytosis

LDL endocytosis, degradation, and receptor recycling are fundamental processes that regulate LDL homeostasis. LDL is a cholesterol-rich lipoprotein particle generated as the end product of VLDL metabolism, a triacylglycerol (triglyceride)-rich lipoprotein particle secreted by the liver. The concentration of plasma LDL is determined by the balance between the rate of biosynthesis and clearance, both of which primarily occur in the liver. More than 80% of circulating LDL is cleared by the liver after cellular internalization of LDL by the LDL receptor (LDLR). Mutations in *LDLR* cause familial hypercholesterolemia (FH), a genetic disease characterized by very high blood cholesterol levels and early onset atherosclerosis. Mutations in other genes including *PCSK9, LDLRAP1* and *APOB* have also been linked to FH. The LDL receptor is a transmembrane glycoprotein that is primarily expressed in hepatocytes and clustered in clathrin-coated pits on the cell surface. Each LDL particle consists of a single apolipoprotein B-100 molecule, the C-terminal region of which is recognized and bound by LDLR for endocytosis. After internalization of the LDL-LDLR complex into a clathrin-coated endocytic vesicle, the coat rapidly disassembles, and LDLR undergoes conformational change induced by endosomal acidity, releasing the LDL ligand. Dissociated LDL particles are transported through early and late endosomes and targeted to the lysosome for hydrolysis, where its cholesterol

content is extracted for cellular metabolism[12]. The majority of ligand-free LDL receptors are transported through the endosomal recycling pathway and recycled back to the plasma membrane to bind and internalize additional LDL particles (Figure 1.1). However, if the LDLR-LDL complex is bound to its negative regulator, proprotein convertase subtilisin/kinexin type 9 (PCSK9), it then fails to undergo conformational change in the endosome, redirecting LDLR to the lysosome along with LDL for degradation[13]. LDLR is also targeted for lysosomal degradation by Inducible Degrader of LDLR (IDOL), a ubiquitin ligase that ubiquinates and marks LDLR for proteasomal degradation[14-16]. Although several regulators of the LDLR recycling pathway have been identified, a complete picture of the mechanism by which LDLR is transported back to the cell surface remains unclear.

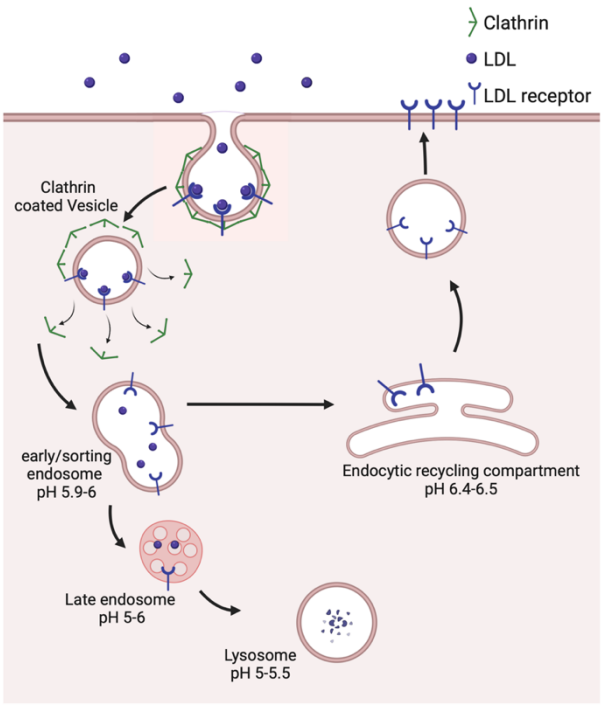

Figure 1.1 Schematic of the endocytic pathway for the LDL-LDLR complex.

LDL binds to LDLR on the cell surface and is endocytosed into clathrin coated vesicles. After internalization, the clathrin complex rapidly dissociates and LDLR releases LDL, which is then transported to the lysosome and hydrolyzed. Free LDLR is then recycled back to the cell surface.

1.2 SREBP mediated regulation of cholesterol biosynthesis and clearance

Cholesterol metabolism is regulated at the transcriptional level by sterol regulatory element-binding proteins (SREBPs), a family of transcription factors that target several genes, including those involved in the biosynthesis and uptake of lipids, e.g., HMG CoA reductase, LDLR, and PCSK9 . SREBP activation is regulated by a negative feedback loop triggered by

sterol concentrations in the endoplasmic reticulum (ER). The precursor form of SREBP complexes with two ER localized proteins, insulin-induced gene (INSIG) and SREBP cleavage-activating protein (SCAP), stabilized by high cellular sterol. Reduced sterol levels in the ER membrane result in ubiquitylation and degradation of INSIG, mediating the release and transport of the SREBP-SCAP complex from the ER to the Golgi[21]. In the Golgi, SREBP is cleaved by two membrane-bound site-1 and -2 proteases (MBTPS1/2), releasing the active N-terminal domain which is then transported to the nucleus to induce target gene expression. LDL-derived cholesterol suppresses the SREBP pathway, creating a feedback mechanism by which cells are able to adjust the production of LDL, LDLR, PCSK9, and other genes to maintain cholesterol homeostasis.

1.3 Lipoprotein(a) (Lp(a)), and it's association with ASCVD

Lp(a) was discovered by Kåre Berg in 1963 as a unique serum lipoprotein[22]. Lp(a) is a variant of LDL, consisting of a core LDL particle bound to an additional protein called apolipoprotein(a) (apo(a)) which makes a single disulfide bond with the apolipoproteinB (apoB)) component of LDL [23, 24](Figure 1.2). An elevated level of Lp(a) in the bloodstream has been linked to atherosclerotic cardiovascular disease as determined by several epidemiologic, genetic, and pathophysiological studies. Lp(a) concentrations above 30–50 mg/dL put an individual at increased risk for a cardiovascular event. Due to the structural similarity of apo(a) to plasminogen, Lp(a) has been hypothesized to be involved in thrombosis by competing for plasminogen binding sites and thereby reducing fibrinolysis. Although many findings link Lp(a) to atherosclerosis and thrombosis, the precise mechanism for its pathogenicity remains unclear. The structure of apo(a) consists of an inactive serine-protease domain and several loop-like kringle (K) domains. The latter include a single copy of the KV and 10 subtypes of the KIV

domain, KIV1-10. KIV subtype 2 is a hypervariable domain that can vary from 1 to >40 repeats. The isoforms of apo(a) encoded by an individual's *LPA* genes determine the size of the Lp(a) particle and have been inversely correlated with Lp(a) plasma level; carriers of low molecular weight isoforms (11-22 KIV repeats) have higher circulating Lp(a) concentrations than carriers of high molecular weight isoforms (>22 KIV repeats). Therefore, copy number polymorphism of *LPA* is a major genetic determinant of Lp(a) concentration and associated disease risk. However, Lp(a) concentrations can vary up to 200-fold between individuals carrying same sized isoforms, suggesting the influence of other types of genetic variation within *LPA*, in addition to copy number length, on Lp(a) concentrations[27]. Indeed, several SNPs in the *LPA* gene have been associated with variation in Lp(a) concentration. A novel and common splice variant of *LPA*, G4925A, occurring predominantly in smaller *LPA* isoforms, was found to be associated with reduced Lp(a) concentrations and lower cardiovascular disease risk, demonstrating the role of other factors in addition to *LPA* size polymorphism in determining blood Lp(a) concentrations [26]. G4925A reduces expression via an undetermined mechanism, distinct from simple loss of function. A second splice variant, G4733A, found in nearly all size-isoforms, though predominantly in medium to large isoforms of *LPA*, is also associated with reduced plasma Lp(a) levels[28-31]. G4733A abolishes a disulfide bond critical for kringle formation, which suggests that an altered protein structure may lower

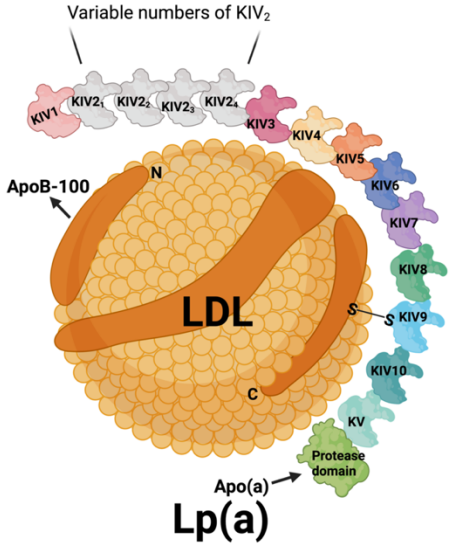

Figure 1.2 Lipoprotein(a) (Lp(a)) structure.

Lp(a) is composed of a core LDL-like particle and a unique protein called apolipoprotein(a) (apo(a)), which is covalently bound to ApoB100 by a single disulfide bond. Apo(a) is encoded by the highly polymorphic *LPA* gene, and contains a protease like domain, one kringle V(KV) domain and 10 different types of kringle IV(KIV) domains. The copy number of KIV subtype 2 can vary from 1->40 repeats.

apo(a) stability leading to reduced Lp(a). Both G4925A and G4733A are thought to reduce the expression of their respective alleles without causing complete protein loss. Several other genetic variants in *LPA* have been associated with reduced Lp(a) concentrations.

1.4 Lp(a) metabolism

Lp(a) is synthesized in the liver, which is also the main site of Lp(a) removal from circulation[33]. Lp(a) particles assemble in a two-step process, with apolipoprotein(a) first forming a noncovalent interaction with the N terminus of apoB-100, which is followed by the formation of a disulfide bond between apo(a) and apoB [34]. The subcellular location of these interactions remains unclear with contradictory data. Studies have shown that plasma concentrations of Lp(a) are regulated not only by the rate of secretion but also by the rate of catabolism[35](Figure 1.3). However, the specific molecular determinants of Lp(a) biosynthesis and catabolism remain largely unknown. In particular, the mechanism of Lp(a) catabolism remains controversial. Several candidate receptors for cellular internalization of Lp(a) have been proposed and tested in vivo and in vitro with inconsistent results. These includes LDLR, very low-density lipoprotein receptor (VLDLR), low density lipoprotein receptor-related protein 1 (LRP1), megalin/gp330, scavenger receptor class B

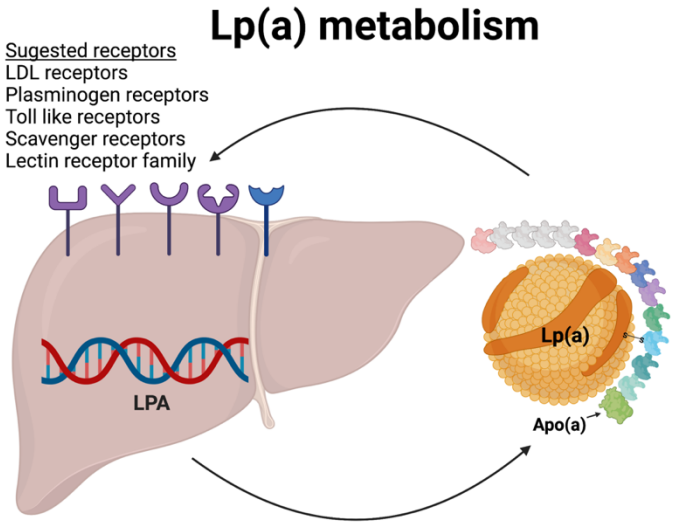

Figure 1.3 Schematic representation of proposed pathway for Lipoprotein(a) (Lp(a)) metabolism.

Lp(a) is synthesized by the liver, where apo(a) is expressed and secreted. Lp(a) assembly may take place either before or after apo(a) secretion. The liver is also the major site of Lp(a) clearance. Several receptors have been proposed to mediate Lp(a) uptake, as illustrated in the figure.

type 1 (SR-B1), Toll like receptor 4, and plasminogen receptors[36, 37]. Due to the structural similarity between LDL and Lp(a), the LDL receptor has been extensively investigated for its potential role in Lp(a) binding and clearance. Lp(a) level is frequently found elevated in familial hypercholesterolemia (FH) patients with complete or partial loss of LDLR function. Interestingly, the two well established LDL-lowering therapies that increase hepatic LDL receptor abundance have different effects on Lp(a) levels. PCSK9 inhibitors, which reduce plasma LDL by 50%-70% by inhibiting LDLR degradation, also reduce plasma concentrations of Lp(a) by 20% to 30% . In contrast, statins, which increase LDLR protein abundance by upregulating *LDLR* gene expression, have no effect on Lp(a) levels[42]. Although their exact mechanism of action remains unclear, recent evidence suggests that PCSK9 inhibitors may reduce Lp(a) concentration by both enhancing clearance[43, 44] and reducing its production and hepatic secretion. Niacin therapy also reduce Lp(a) levels by amounts similar to that of the PCSK9 inhibitors, but by an unknown mechanism, and with no known effect on LDLR. Thus, the contribution of LDLR to lipoprotein(a) removal remains unclear. This uncertainty has led to a lack of therapeutic approaches for lowering Lp(a) concentrations, with current strategies in development instead targeting LPA gene expression.

1.5 Concluding remarks

Atherosclerotic cardiovascular diseases (ASCVD), linked to elevated levels of LDL, are the leading causes of mortality and morbidity worldwide. A critical pathway regulating plasma LDL is mediated by LDLR expressed on the liver cell surface, with LDLR binding and mediating the endocytosis of circulating LDL particles. LDLR, the major therapeutic target for lowering atherogenic plasma LDL, has been extensively investigated. Despite a sophisticated

understanding of LDLR synthesis and endocytosis, the factors regulating the recycling of LDLR remain largely unknown.

Elevated plasma Lp(a) is another factor independently linked to ASCVD with proinflammatory, proatherogenic and potentially prothrombotic properties. The concentration of Lp(a) in the plasma of an individual is largely genetically determined. *LPA* was identified more than 40 years ago and has emerged as a clinically important molecule in recent years. Yet after decades of research, information regarding the assembly, clearance and catabolism of Lp(a) remains controversial, which has limited the development of Lp(a)-lowering therapeutics.

1.6 References

1. Brown, M.S. and J.L. Goldstein, The SREBP pathway: regulation of cholesterol metabolism by proteolysis of a membrane-bound transcription factor. Cell, 1997. 89(3): p. 331-40.
2. Eberlé, D., et al., SREBP transcription factors: master regulators of lipid homeostasis. Biochimie, 2004. 86(11): p. 839-48.
3. Jeong, H.J., et al., Sterol-dependent regulation of proprotein convertase subtilisin/kexin type 9 expression by sterol-regulatory element binding protein-2. J Lipid Res, 2008. 49(2): p. 399-409.
4. Yabe, D., M.S. Brown, and J.L. Goldstein, Insig-2, a second endoplasmic reticulum protein that binds SCAP and blocks export of sterol regulatory element-binding proteins. Proc Natl Acad Sci U S A, 2002. 99(20): p. 12753-8.
5. Yang, T., et al., Crucial step in cholesterol homeostasis: sterols promote binding of SCAP to INSIG-1, a membrane protein that facilitates retention of SREBPs in ER. Cell, 2002. 110(4): p. 489-500.
6. Sun, L.P., et al., Insig required for sterol-mediated inhibition of Scap/SREBP binding to COPII proteins in vitro. J Biol Chem, 2005. 280(28): p. 26483-90.
7. Berg, K., A NEW SERUM TYPE SYSTEM IN MAN--THE LP SYSTEM. Acta Pathol Microbiol Scand, 1963. 59: p. 369-82.
8. Utermann, G. and W. Weber, Protein composition of Lp(a) lipoprotein from human plasma. FEBS Lett, 1983. 154(2): p. 357-61.
9. Tsimikas, S., et al., NHLBI Working Group Recommendations to Reduce Lipoprotein(a)-Mediated Risk of Cardiovascular Disease and Aortic Stenosis. J Am Coll Cardiol, 2018. 71(2): p. 177-192.
10. Kamstrup, P.R. and B.G. Nordestgaard, Elevated Lipoprotein(a) Levels, LPA Risk Genotypes, and Increased Risk of Heart Failure in the General Population. JACC Heart Fail, 2016. 4(1): p. 78-87.

11. Kronenberg, F., Human Genetics and the Causal Role of Lipoprotein(a) for Various Diseases. Cardiovasc Drugs Ther, 2016. 30(1): p. 87-100.
12. Nordestgaard, B.G., et al., Lipoprotein(a) as a cardiovascular risk factor: current status. Eur Heart J, 2010. 31(23): p. 2844-53.
13. Perombelon, Y.F., A.K. Soutar, and B.L. Knight, Variation in lipoprotein(a) concentration associated with different apolipoprotein(a) alleles. J Clin Invest, 1994. 93(4): p. 1481-92.
14. Coassin, S., et al., A novel but frequent variant in LPA KIV-2 is associated with a pronounced Lp(a) and cardiovascular risk reduction. Eur Heart J, 2017. 38(23): p. 1823-1831.
15. Schachtl-Riess, J.F., et al., Frequent LPA KIV-2 Variants Lower Lipoprotein(a) Concentrations and Protect Against Coronary Artery Disease. J Am Coll Cardiol, 2021. 78(5): p. 437-449.
16. Schmidt, K., et al., Structure, function, and genetics of lipoprotein (a). J Lipid Res, 2016. 57(8): p. 1339-59.
17. Morgan, B.M., et al., Nonsynonymous SNPs in LPA homologous to plasminogen deficiency mutants represent novel null apo(a) alleles. J Lipid Res, 2020. 61(3): p. 432-444.
18. Di Maio, S., et al., Investigation of a nonsense mutation located in the complex KIV-2 copy number variation region of apolipoprotein(a) in 10,910 individuals. Genome Med, 2020. 12(1): p. 74.
19. Coassin, S. and F. Kronenberg, Lipoprotein(a) beyond the kringle IV repeat polymorphism: The complexity of genetic variation in the LPA gene. Atherosclerosis, 2022. 349: p. 17-35.
20. Cain, W.J., et al., Lipoprotein [a] is cleared from the plasma primarily by the liver in a process mediated by apolipoprotein [a]. J Lipid Res, 2005. 46(12): p. 2681-91.
21. McCormick, S.P.A. and W.J. Schneider, Lipoprotein(a) catabolism: a case of multiple receptors. Pathology, 2019. 51(2): p. 155-164.
22. Alonso, R., et al., Lipoprotein(a) levels in familial hypercholesterolemia: an important predictor of cardiovascular disease independent of the type of LDL receptor mutation. J Am Coll Cardiol, 2014. 63(19): p. 1982-9.
23. Durrington, P.N., et al., Lipoprotein (a) in familial hypercholesterolaemia. Curr Opin Lipidol, 2022.
24. Alonso, R., et al., PCSK9 and lipoprotein (a) levels are two predictors of coronary artery calcification in asymptomatic patients with familial hypercholesterolemia. Atherosclerosis, 2016. 254: p. 249-253.
25. Lambert, G., et al., The complexity of lipoprotein (a) lowering by PCSK9 monoclonal antibodies. Clin Sci (Lond), 2017. 131(4): p. 261-268.
26. Reyes-Soffer, G., et al., Effects of PCSK9 Inhibition With Alirocumab on Lipoprotein Metabolism in Healthy Humans. Circulation, 2017. 135(4): p. 352-362.
27. de Boer, L.M., et al., Statin therapy and lipoprotein(a) levels: a systematic review and meta-analysis. Eur J Prev Cardiol, 2022. 29(5): p. 779-792.
28. Watts, G.F., et al., Controlled study of the effect of proprotein convertase subtilisin-kexin type 9 inhibition with evolocumab on lipoprotein(a) particle kinetics. Eur Heart J, 2018. 39(27): p. 2577-2585.

29. Croyal, M., et al., PCSK9 inhibition with alirocumab reduces lipoprotein(a) levels in nonhuman primates by lowering apolipoprotein(a) production rate. Clin Sci (Lond), 2018. 132(10): p. 1075-1083.
30. Tsimikas, S., et al., Lipoprotein(a) Reduction in Persons with Cardiovascular Disease. N Engl J Med, 2020. 382(3): p. 244-255.
31. Sheridan, C., RNA drugs lower lipoprotein(a) and genetically driven cholesterol. Nat Biotechnol, 2022. 40(7): p. 983-985.
32. Dashti, M., et al., A phospholipidomic analysis of all defined human plasma lipoproteins. Sci Rep, 2011. 1: p. 139.
33. Segrest, J.P., et al., Structure of apolipoprotein B-100 in low density lipoproteins. J Lipid Res, 2001. 42(9): p. 1346-67.
34. Ivanova, E.A., et al., Small Dense Low-Density Lipoprotein as Biomarker for Atherosclerotic Diseases. Oxid Med Cell Longev, 2017. 2017: p. 1273042.
35. Ahotupa, M., Oxidized lipoprotein lipids and atherosclerosis. Free Radic Res, 2017. 51(4): p. 439-447.
36. Staprans, I., et al., Oxidized lipids in the diet are incorporated by the liver into very low density lipoprotein in rats. J Lipid Res, 1996. 37(2): p. 420-30.
37. Stocker, R. and J.F. Keaney, Jr., Role of oxidative modifications in atherosclerosis. Physiol Rev, 2004. 84(4): p. 1381-478.
38. Rader, D.J., J. Cohen, and H.H. Hobbs, Monogenic hypercholesterolemia: new insights in pathogenesis and treatment. J Clin Invest, 2003. 111(12): p. 1795-803.
39. Yang, H.X., et al., Cholesterol in LDL receptor recycling and degradation. Clin Chim Acta, 2020. 500: p. 81-86.
40. Horton, J.D., J.C. Cohen, and H.H. Hobbs, Molecular biology of PCSK9: its role in LDL metabolism. Trends Biochem Sci, 2007. 32(2): p. 71-7.
41. Zhang, C.P., et al., IDOL, inducible degrader of low-density lipoprotein receptor, serves as a potential therapeutic target for dyslipidemia. Med Hypotheses, 2016. 86: p. 138-42.
42. Zhang, L., et al., The IDOL-UBE2D complex mediates sterol-dependent degradation of the LDL receptor. Genes Dev, 2011. 25(12): p. 1262-74.
43. Emmer, B.T., et al., Genome-scale CRISPR screening for modifiers of cellular LDL uptake. PLoS Genet, 2021. 17(1): p. e1009285.
44. Goldstein, J.L. and M.S. Brown, A century of cholesterol and coronaries: from plaques to genes to statins. Cell, 2015. 161(1): p. 161-172.
45. Pietiäinen, V., et al., NDRG1 functions in LDL receptor trafficking by regulating endosomal recycling and degradation. J Cell Sci, 2013. 126(Pt 17): p. 3961-71.
46. Brown, M.S. and J.L. Goldstein, Receptor-mediated endocytosis: insights from the lipoprotein receptor system. Proc Natl Acad Sci U S A, 1979. 76(7): p. 3330-7.

Chapter 2 The Small GTPase RAB10 Regulates Endosomal Recycling of the LDL Receptor and Transferrin Receptor in Hepatocytes[1]

Abstract

The low-density lipoprotein receptor (LDLR) mediates the hepatic uptake of circulating low-density lipoproteins (LDL), a process that modulates the development of atherosclerotic cardiovascular disease. We recently identified *RAB10*, encoding a small GTPase, as a positive regulator of LDL uptake in hepatocellular carcinoma cells (HuH7) in a genome-wide CRISPR screen, though the underlying molecular mechanism for this effect was unknown. We now report that RAB10 regulates hepatocyte LDL uptake by promoting the recycling of endocytosed LDLR from RAB11-positive endosomes to the plasma membrane. We also show that RAB10 similarly promotes the recycling of the transferrin receptor, which binds the transferrin protein that mediates the transport of iron in the blood, albeit from a distinct RAB4-positive compartment. Taken together, our findings suggest a model in which RAB10 regulates LDL and transferrin uptake by promoting both slow and rapid recycling routes for their respective receptor proteins.

2.1 Introduction

An elevated level of circulating low-density lipoprotein (LDL) cholesterol is a major risk factor for atherosclerotic cardiovascular diseases, including myocardial infarction and stroke.

---

[1] This chapter is reproduced from Khan, T. G., Ginsburg, D., and Emmer, B. T. The small GTPase RAB10 regulates endosomal recycling of the LDL receptor and transferrin receptor in hepatocytes. *J Lipid Res* (2022) 63(8) 100248, DOI: 10.1016/j.jlr.2022.100248

Regulation of plasma cholesterol is governed by a complex interplay between dietary absorption, de novo biosynthesis, and clearance from the bloodstream. Therapeutic targeting of LDL clearance has been a highly successful strategy for the prevention and treatment of atherosclerosis. LDL clearance is mediated by the LDL receptor (LDLR), a cell surface glycoprotein that directly binds to the apolipoprotein B component of LDL particles and triggers clathrin-mediated endocytosis. The acidic environment of the endosomal lumen induces complex dissociation, with LDL subsequently transported to the lysosome for hydrolysis, and free LDLR recycled back to the plasma membrane. Many regulatory proteins affecting the endocytic pathway and cell surface expression of LDLR have been identified, including PCSK9, a negative regulator that redirects LDLR to the lysosome for degradation [3, 11], and IDOL, a ubiquitin ligase that induces proteasomal degradation of LDLR . Although much is known about the regulation of LDLR expression and endocytosis, questions remain concerning the molecular determinants of LDLR recycling.

We recently reported a genome-wide CRISPR screen for modifiers of LDL uptake in HuH7 cells [2, 4, 7, 13-16]. This screen identified RAB10, a small GTPase known to mediate trafficking of vesicles between intracellular compartments, as a key regulator of LDL uptake. Deletion of *RAB10* decreased cellular endocytosis of LDL but increased accumulation of another endocytic cargo, transferrin. The receptors for low-density lipoprotein (LDLR) and transferrin (TFR) are both endocytosed from the cell surface via clathrin coated vesicles and transported through intracellular recycling pathways . In this study, we investigated the role of RAB10 in LDL and transferrin endocytosis. Our results demonstrate that GTP-bound RAB10 positively regulates the activity of LDLR and TFR by accelerating the recycling of both proteins to the plasma membrane.

2.2 Results

RAB10 regulates the cellular uptake of LDL and transferrin

To test the influence of RAB10 on LDL uptake, we generated RAB10 deficient HuH7 cells by CRISPR-mediated disruption of the *RAB10* gene and confirmed efficient depletion of RAB10 protein by immunoblotting (Fig 2.1A). Consistent with the findings of our previous CRISPR screen [11, 18, 19], *RAB10*-targeted cells exhibited decreased uptake of fluorescently-labeled LDL and increased accumulation of fluorescently-labeled transferrin relative to control cells treated with a non-targeting gRNA (Fig 2.1B, 2.1C). To rule out a CRISPR off-target effect, we transduced *RAB10*-targeted cells with a lentivirus directing expression of *RAB10* cDNA with a synonymous mutation conferring resistance to CRISPR disruption; this heterologous expression of wild-type *RAB10* cDNA rescued LDL and transferrin uptake, confirming that the observed effects of *RAB10*-targeting were mediated by

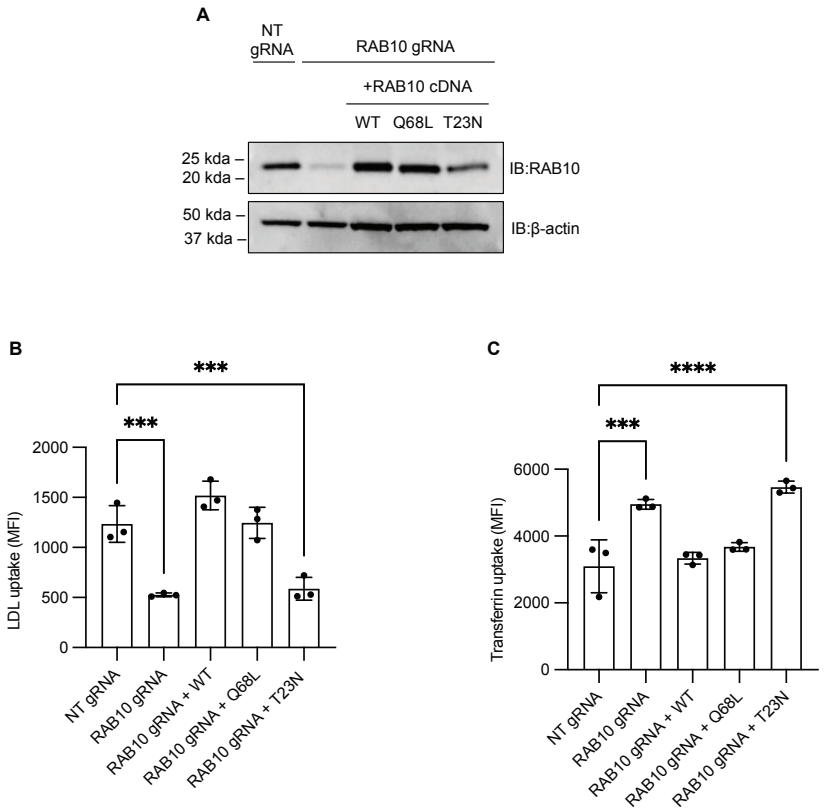

Figure 2.1 RAB10 exhibits opposite effects on cellular accumulation of LDL and transferrin.

(A) Immunoblotting of lysates prepared from HuH7 cells treated with a control nontargeting (NT) gRNA or a gRNA targeting RAB10, with or without heterologous expression of a CRISPR-resistant wild-type (WT), GTP-locked (Q68L), or GDP-locked (T23N) RAB10 cDNA. (B-C) Fold change of internalized fluorescent LDL (B) or transferrin (C) relative to NT control for cells indicated in (A). Individual data points represent independent biologic replicates, error bars indicate standard deviation, * p-value <0.01 (one-way ANOVA test).

on-target activity (Fig 2.1B, 2.1C). We also tested the requirement of GTPase cycling for RAB10 function in LDL and transferrin uptake by expressing RAB10 point mutants locked in the GTP-bound or GDP-bound states (Fig 2.1A). Expression of both wild type and GTP-locked RAB10 (Q68L) rescued the LDL (Fig 2.1B) and transferrin (Fig 2.1C) uptake phenotype of *RAB10*-targeted cells, whereas expression of GDP-locked RAB10 (T23N) had no effect.

RAB10 regulates the cellular distribution of LDLR and TFR

To clarify the molecular basis for altered LDL and transferrin uptake in *RAB10*-deficient cells, we analyzed the total protein abundance and surface expression for the corresponding cellular receptors, LDLR[21] and TFR[4, 17]. Despite the decreased LDL uptake observed in *RAB10*-targeted cells (Fig 2.1B), these same cells exhibited increased levels of total cellular LDLR protein, as measured by both immunoblotting (Fig 2.2A, 2.2B) and by flow cytometry of permeabilized cells (Fig 2.2C), with no corresponding change in LDLR transcript levels by qRT-PCR (Fig 2.2D). This increase in total cellular LDLR protein but not mRNA in *RAB10*-targeted cells suggested that the observed decrease in LDL uptake by these cells was due to a defect in either LDLR trafficking or activity rather than an effect on LDLR gene expression. Indeed, flow cytometry of non-permeabilized RAB10-targeted cells demonstrated a redistribution of cellular LDLR protein from the cell surface to intracellular compartments (Fig 2.2E, Supplementary Fig 2.1A). In contrast, overexpression of either wild-type or GTP-locked RAB10 had the opposite effect, increasing the proportion of LDLR at the cell surface (Supplementary Fig 2.1B).

To examine the effects of RAB10 on TFR, we similarly analyzed the distribution of TFR in *RAB10*-targeted cells. Despite the divergent effects of *RAB10*-targeting on LDL and

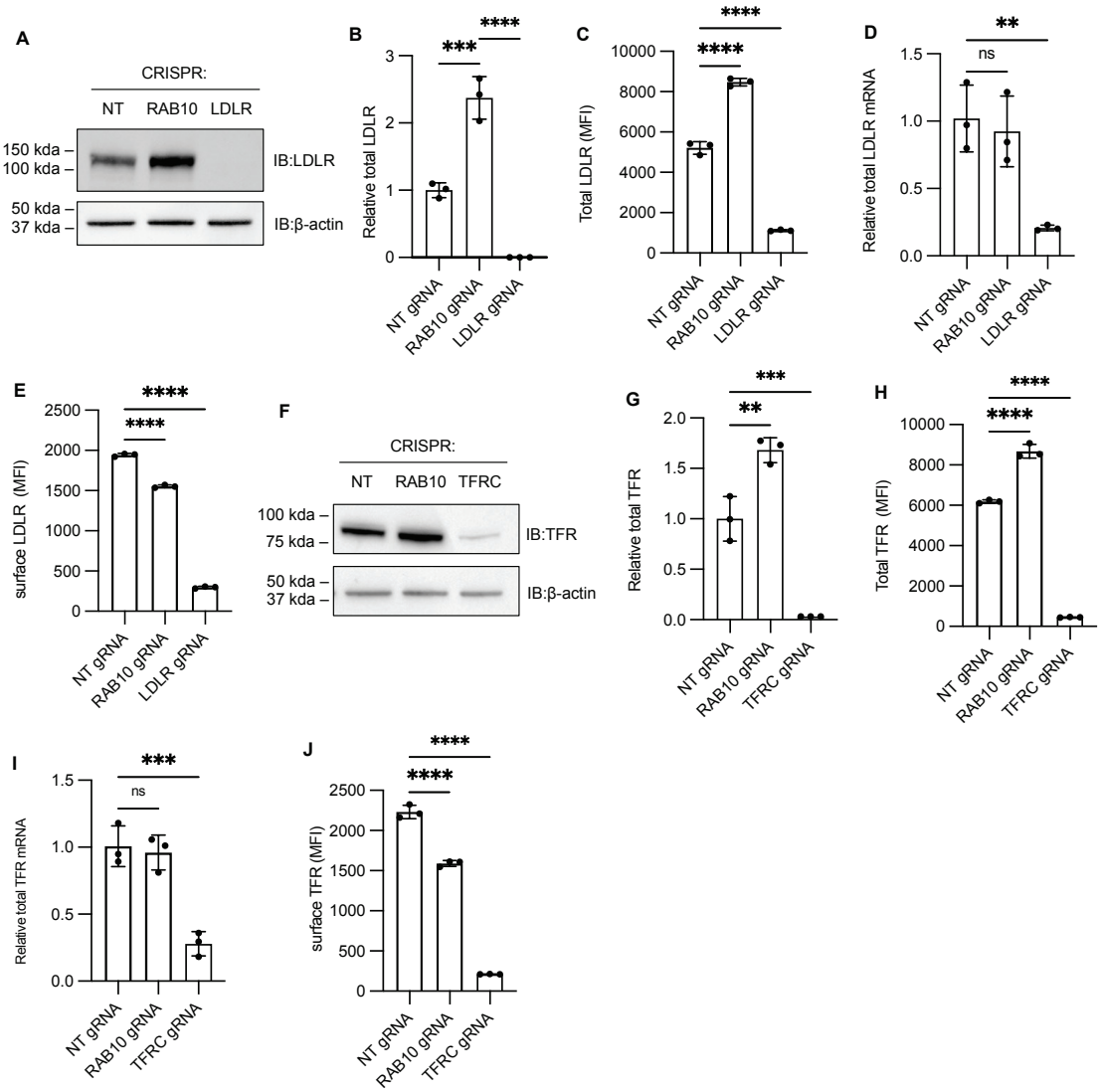

Figure 2.2 RAB10 regulates cell surface expression of LDLR and TFR.

HuH7 cells were treated with a gRNA targeting RAB10, LDLR, TFRC, or a nontargeting (NT) control. Changes in LDLR (A-E) and TFR (F-J) were evaluated by western blotting (A-B, F-G) or flow cytometry of permeabilized cells (C, H) for total cellular protein, flow cytometry of intact cells for surface-displayed protein (E, J), or qRT-PCR for mRNA abundance (D, I). Individual data points represent independent biologic replicates, error bars indicate standard deviation, * p-value <0.01 (one-way ANOVA test).

transferrin uptake (Fig 2.1B, 2.1C), the effect on TFR abundance mirrored its effect on LDLR, with total cellular TFR protein levels increased (Fig 2.2F-H) while mRNA levels were unchanged (Fig 2.2I) and surface-displayed protein levels were reduced (Fig 2.2J). These

similarities suggest that the discordant effects of *RAB10* targeting on LDL and transferrin cellular accumulation are a result of different fates of the labeled ligand rather than their corresponding receptors. Consistent with this interpretation, internalized LDL is released from LDLR in acidic compartments whereas transferrin remains in complex with TFR until it is released to the extracellular environment after TFR is recycled back to the plasma membrane .

Heterogeneous distribution of RAB10 in subcellular compartments

We next assessed the localization of RAB10 in HuH7 cells by immunofluorescence microscopy. Staining of *RAB10*-targeted cells confirmed the specificity of the RAB10 antibody (Fig 2.3A). We observed colocalization of RAB10 with markers of the early endosome (EEA1), recycling endosome (RAB11), trans-Golgi network (TGN46), and endoplasmic reticulum (ER, PDI) (Fig 2.3B), consistent with prior studies of RAB10 in other cell types . We quantified the relative distribution of RAB10 in these intracellular compartments and observed that RAB10 was sparsely distributed in EEA1-positive early endosomes and in the TGN46-positive trans-Golgi network. We also observed a large pool of RAB10 colocalized with RAB11-positive recycling endosomes and with the PDI-positive ER (Fig 2.3C). We next tested how the GTPase cycle of RAB10 affected its localization by comparison of wild-type, GTP-locked (Q68L), or GDP-locked (T23N) RAB10 expressed in a clonal cell line deleted for endogenous RAB10 (Fig 2.3D). Consistent with previous reports , we observed significantly decreased steady state protein levels for the GDP-locked mutant by both immunoblotting (Fig 2.3D) and immunofluorescence (Fig 2.3E). In contrast, steady state levels of the GTP-locked (Q68L) mutant were comparable to those of wild-type RAB10 (Fig 2.3D, 2.3E). In comparison to wild-type RAB10, GTP-locked RAB10 demonstrated increased colocalization with TGN46 and decreased colocalization with Rab11 (Fig. 2.3F, G). Together, these findings highlight the heterogeneous subcellular

distribution of RAB10, its modulation by the GTPase cycle, and its potential to directly regulate the vesicular trafficking of LDLR and TFR.

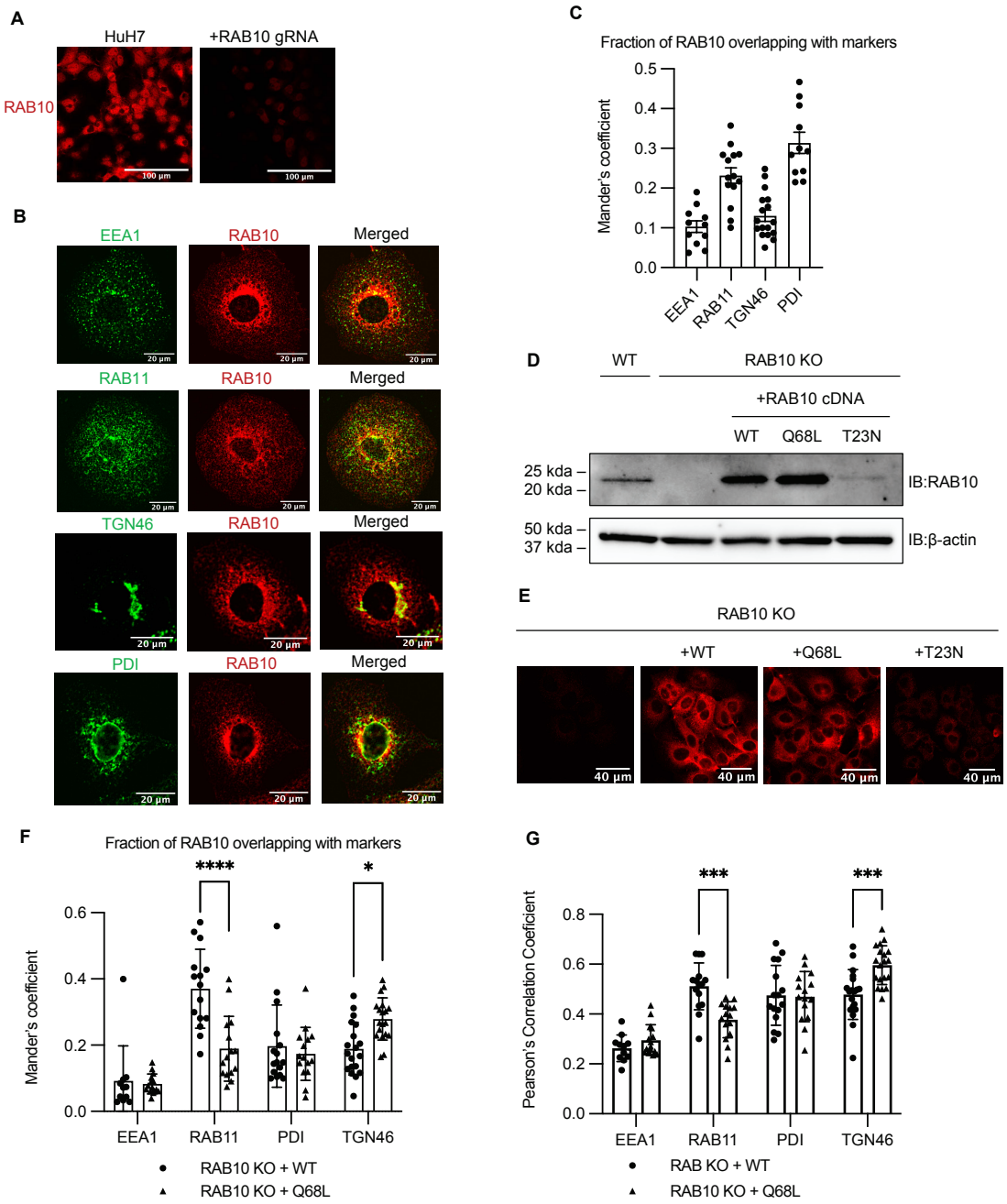

Figure 2.3 Characterization of subcellular localization of RAB10.

(A) RAB10 immunofluorescence of wild-type and RAB10-targeted HuH7 cells. (B) Co-staining of wild type HuH7 cells for RAB10 and the indicated markers for different subcellular compartments. (C) Mander's coefficient showing overlap of endogenous RAB10 with the indicated marker in HuH7 cells. (D) Western blot of lysates prepared from wild-type and a RAB10-deleted HuH7 clonal cell line with or without heterologous expression of wild type, Q68L, or T23N CRISPR-resistant RAB10 cDNA. (E) RAB10 immunoflourescence of the cells indicated in (D). (F-G) Mander's coefficient and Pearson's correlation coefficient for the colocalization of the indicated marker with wild type or Q68L RAB10. Individual data points represent single cells imaged in two to three biological replicates; error bars indicate standard deviation. * p-value<0.01 (two-way ANOVA).

RAB10 depletion induces the redistribution of LDLR and TFR within subcellular compartments

By confocal imaging we observed that a subset of RAB10 colocalized with both LDLR and TFR in intracellular punctae, (Supplementary Fig 2.2A, 2.2B). We examined the impact of RAB10 depletion on the intracellular distribution of LDLR and TFR. Consistent with the cellular accumulation of LDLR and TFR in *RAB10*-targeted cells detected by immunoblotting and flow cytometry (Fig 2.2A-C, F-H), immunofluorescence of *RAB10*-targeted cells revealed increased staining for both LDLR and TFR that remained distributed in punctae (Fig 2.4). Colocalization analysis revealed the intracellular accumulation of LDLR to occur primarily in RAB11-positive recycling endosomes in *RAB10*-deleted cells (Fig. 2.4C, 2.4H), consistent with a role for RAB10 in receptor recycling, with no change in colocalization with the early endosomal marker EEA1(Fig. 2.4A, 2.4H), the early endosomal/rapid recycling marker RAB4 (Fig. 2.4B, 2.4H), the cis-Golgi marker GM130(Fig. 2.4E, 2.4H), the ER marker PDI(Fig. 2.4F, 2.4H), or the lysosomal marker Lamp1(Fig. 2.4G, 2.4H). Significant LDLR accumulation was also observed in the trans-Golgi network, as reflected by TGN46 colocalization (Fig. 2.4D, 2.4H).

A similar analysis of TFR redistribution in *RAB10*-targeted cells revealed a significant increase in colocalization with RAB4 (Fig. 2.5B, 2.5G) and a reduced colocalization with EEA1 (Fig. 2.5A, 2.5G). In contrast to LDLR, no significant increase in colocalization was observed for TFR with Rab11 and TGN46 (Fig. 2.5C-D, 2.5G). Similar to LDLR, no change in TFR colocalization was observed for markers of the cis-Golgi network (Fig. 2.5E, 2.5G) or the ER (Fig. 2.5F, 2.5G). These findings suggest that RAB10 depletion affects distribution of LDLR and TFR in distinct recycling compartments.

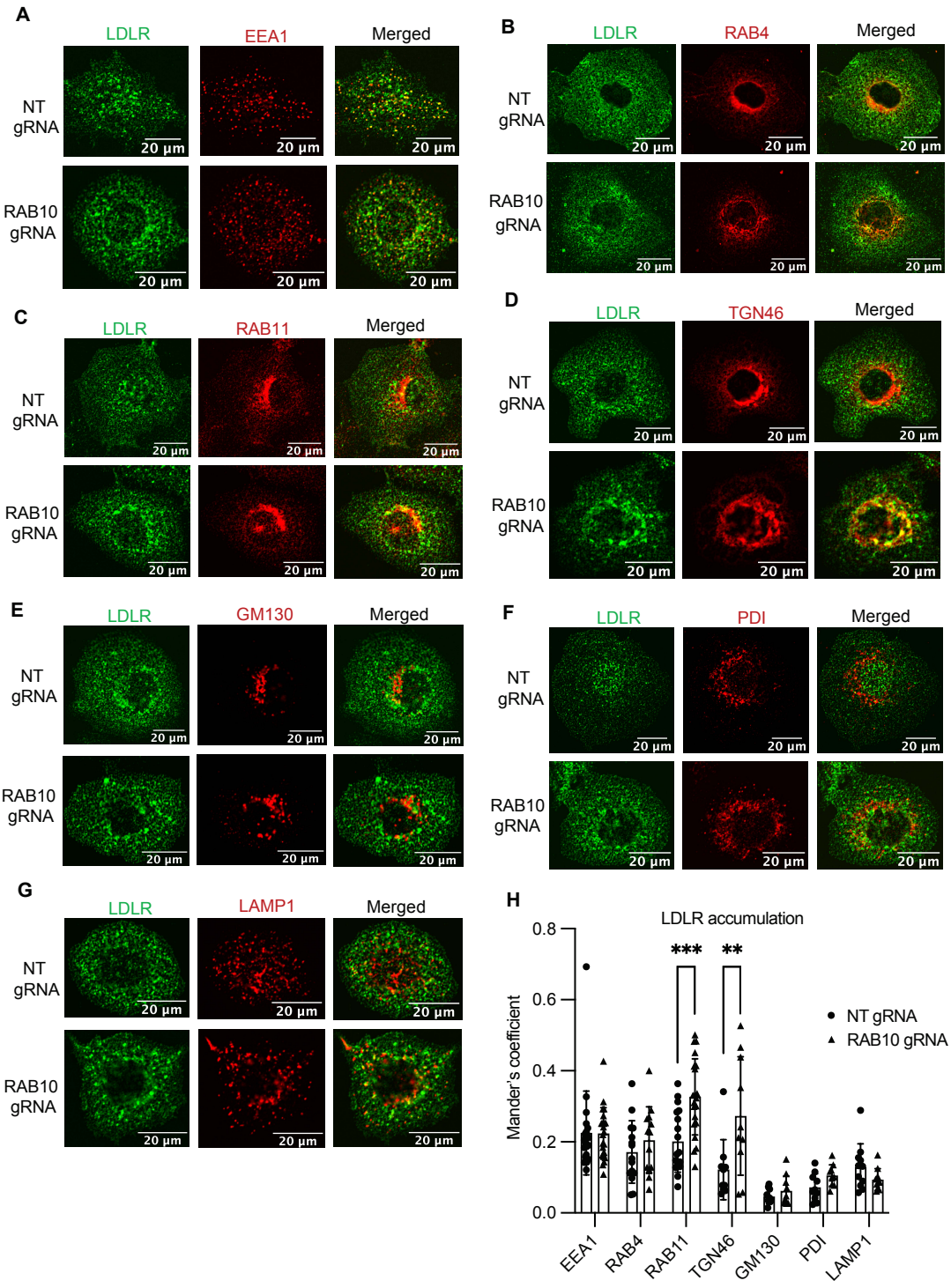

Figure 2.4 RAB10 deletion alters LDLR intracellular distribution.

(A-G) HuH7 cells treated with either a RAB10-targeting gRNA or a non-targeting control (NT) were co-stained for LDLR and intracellular compartment markers EEA1(A), RAB4(B), RAB11(C), TGN46(D), GM130(E), PDI(F) or LAMP1(G). (H) Mander's overlap of LDLR with each indicated marker. Individual data points represent single cells imaged in two to three biological replicates; error bars indicate standard deviation. * p-value<0.01 (two-way ANOVA)

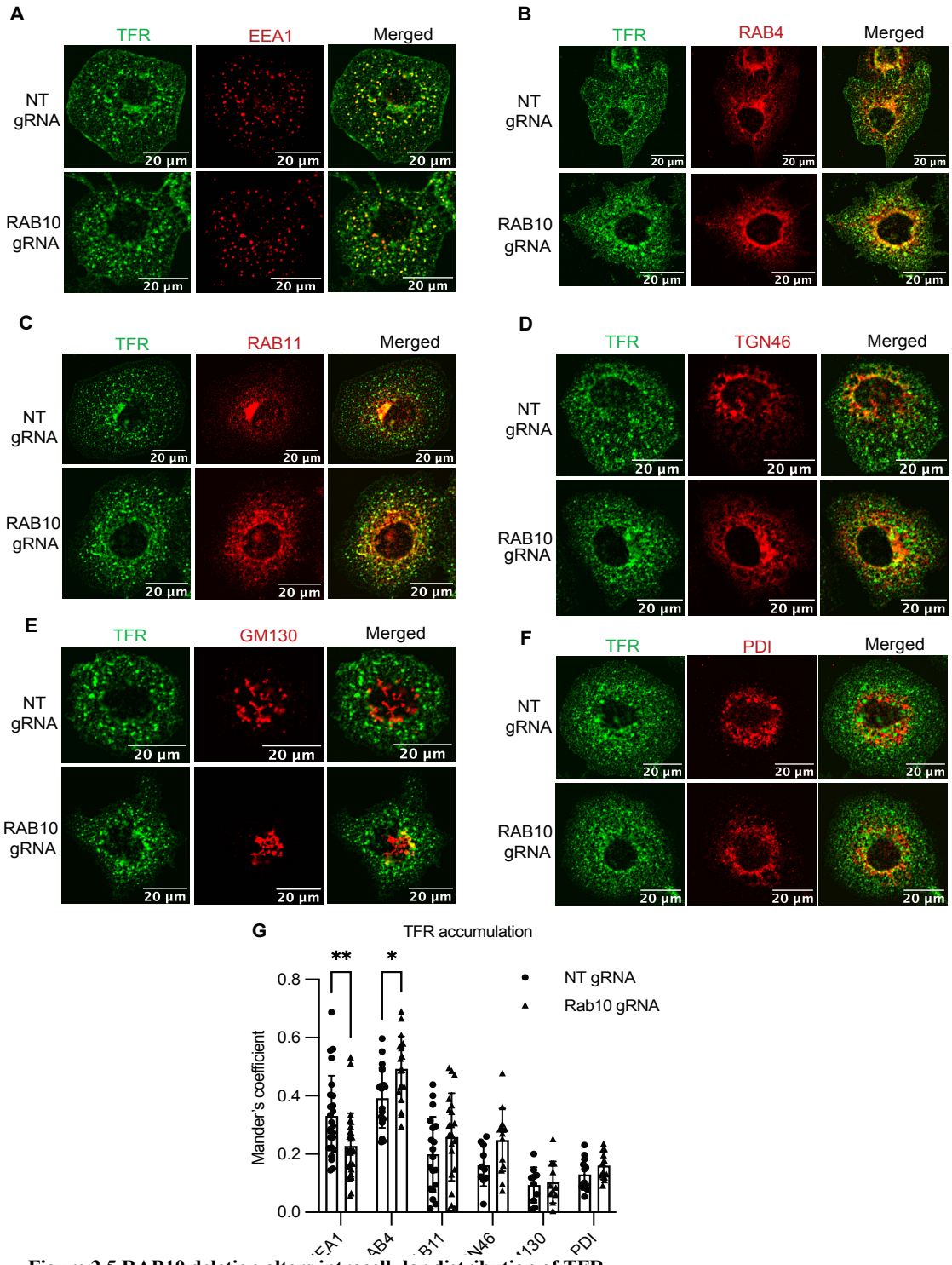

Figure 2.5 RAB10 deletion alters intracellular distribution of TFR.

(A-F) HuH7 cells treated with either a *RAB10*-targeting gRNA or non-targeting control (NT) were co-stained for TFR and intracellular compartment markers EEA1(A), RAB4(B), RAB11(C), TGN46(D), GM130(E), and PDI(F). (G) Mander's overlap of TFR with each indicated marker. Individual data points represent single cells imaged in two to three biological replicates; error bars indicate standard deviation. * p-value< 0.01 (two-way ANOVA).

RAB10 does not alter the kinetics of endocytosis for LDLR or TFR

The redistribution of LDLR and TFR from the plasma membrane to endosomes in *RAB10*-targeted cells could be due to an influence on endocytosis or recycling. To distinguish between these possibilities, we first examined endocytosis of TFR in complex with fluorescently labeled transferrin in *RAB10*-targeted and control cells using a previously reported approach . Briefly, cell surface TFR was saturated with fluorescently conjugated transferrin, with samples cooled to 4°C to block endocytosis. Endocytosis was then induced by increasing the temperature to 37°C for various intervals, after which the temperature was again rapidly lowered to 4°C and remaining surface bound transferrin was removed by washing with acidic buffer. Internalized TFR-transferrin complex was then quantified by flow cytometry. At time zero, less fluorescent transferrin was bound to *RAB10*-depleted cells compared to control cells (Fig. 2.6A), consistent with the decreased surface TFR abundance in *RAB10*-targeted cells by flow cytometry (Fig. 2.2J). For the fluorescent transferrin that was bound to the cell surface, internalization was complete within 5-10 minutes, with no significant difference in the rate of endocytosis between *RAB10*-depleted and control cells (Fig. 2.6B).

In contrast to the TFR-transferrin complex, LDLR-LDL dissociates in the acidic environment of early endosomes with subsequent LDL degradation , which limits the utility of fluorescent LDL to monitor endocytosis. We therefore used an antibody that recognizes an LDLR extracellular epitope to assay LDLR endocytosis kinetics . Cell surface LDLR was first saturated with LDLR antibody at 4°C, with endocytosis then triggered by a temperature shift to 37°C. Samples taken at different time points were then quickly chilled to block further endocytosis and the remaining surface LDLR-antibody complex was stained with fluorescently labelled secondary antibody, with the fraction of internalized LDLR antibody reflected by its

protection from surface staining with secondary antibody. Consistent with decreased surface LDLR in *RAB10* depleted cells, less fluorescent antibody was bound at time zero compared to control cells (Fig 2.2E, Fig. 2.6C). Similar to TFR, no difference was observed in the rate of LDLR endocytosis between control and *RAB10*-depleted cells (Fig. 2.6D).

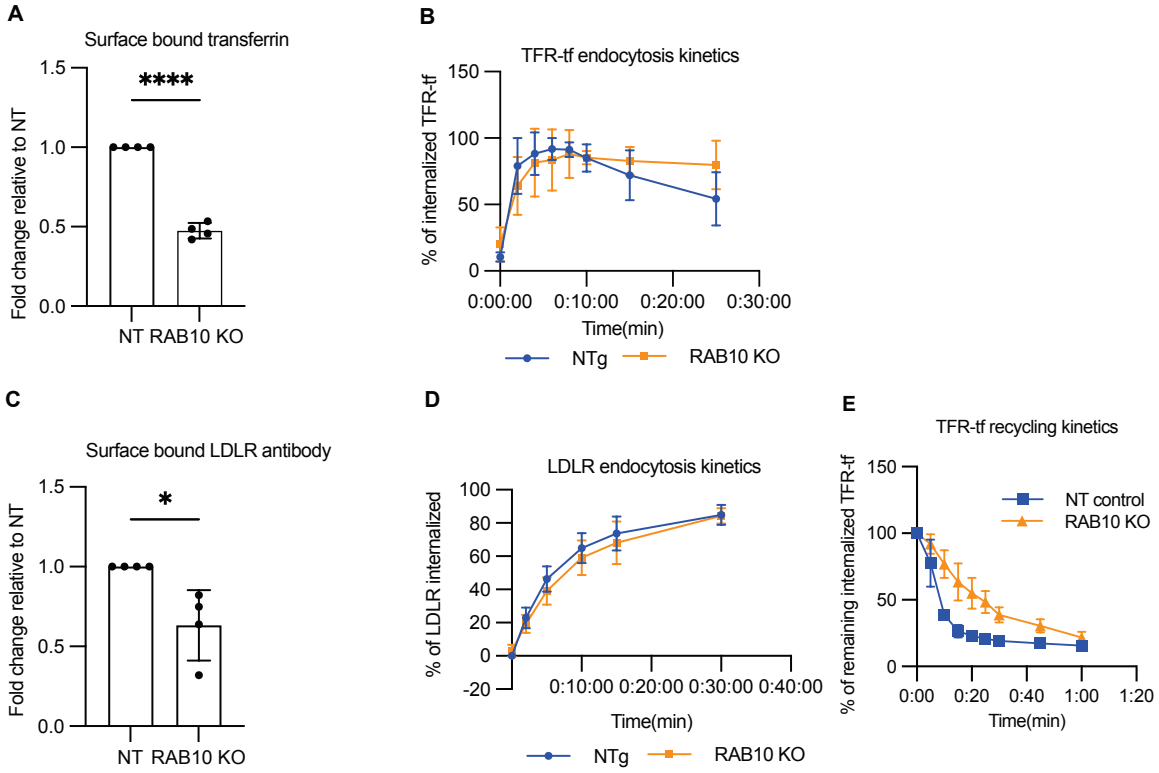

Figure 2.6 RAB10 regulates recycling but not endocytosis.

(A-B) HuH7 cells transduced with a RAB10-targeting gRNA or non-targeting gRNA control (NT) were assessed for surface binding of transferrin at time 0 (A) and at serial time points following endocytosis for internalization of surface-bound transferrin (B) by flow cytometry. (C-D) Surface-exposed LDLR was labeled with fluorescent antibody and assayed for internalization after various time points by flow cytometry. (E) TFR recycling was assayed by synchronizing cells with internalized transferrin and tracking the reduction in fluorescent signal at indicated time points by flow cytometry. Error bars represent standard deviation for 4 biologic replicates. * p-value <0.01 (student's t-test)

RAB10 promotes the recycling of TFR

In our assay of TFR endocytosis (Fig 2.6B), we noted a trend toward a decrease in cellular fluorescence after 10 minutes in control cells that was less pronounced in *RAB10*-depleted cells. This time frame is consistent with what would be expected for bulk recycling of endocytosed receptor from common endosomes . We thus examined the recycling kinetics of TFR in response

to RAB10 depletion. Cells were loaded with fluorescent transferrin at 37°C for 30 minutes, endocytosis was then blocked by cold treatment, and recycling was induced by shifting samples to 37°C for different chase periods. Samples of cells at specific time points were quickly chilled and resurfaced TFR-transferrin was acid-washed. Remaining intracellular TFR-transferrin was then quantified by flow cytometry. *RAB10*-targeting resulted in a significant delay in TFR recycling, with 50% of the intracellular transferrin-TFR complexes recycled within 8 minutes for control cells compared to 15-20 minutes for *RAB10*-targeted cells (Fig. 2.6E).

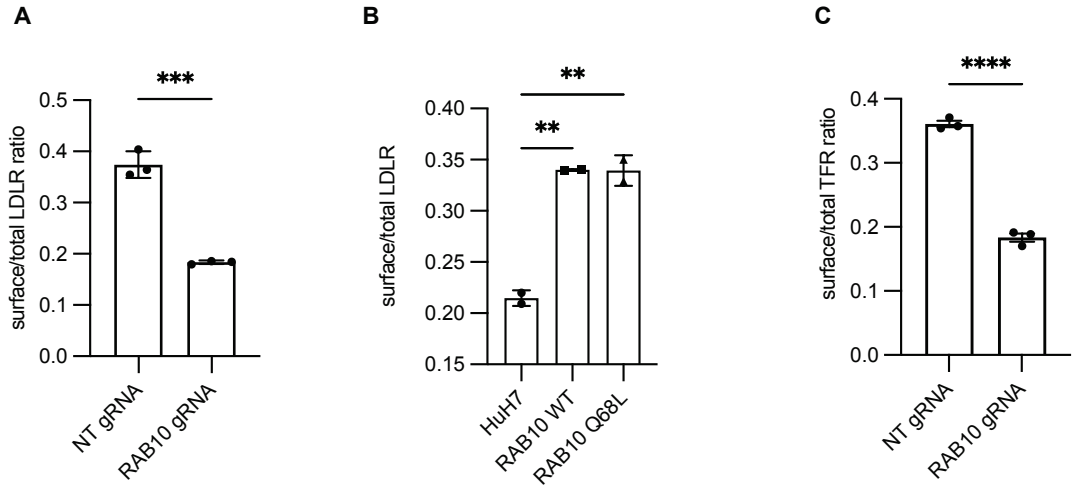

Figure 2.7 RAB10 regulates the ratio of surface to total LDLR and TFR.

(A) Ratio of surface to total LDLR abundance for HuH7 cells treated with a gRNA targeting *RAB10*, or a nontargeting (NT) control. *** p-value <0.0002 (student's t-test). (B) Ratio of surface to total LDLR abundance for wild-type HuH7 cells and HuH7 cells overexpressing wild-type or the Q68L mutant of RAB10. **p-value = 0.0017 (one-way ANOVA). (C) Ratio of surface to total TFR abundance for HuH7 cells treated with a *RAB10*-targeting gRNA or NT control. **** p-value <0.0001 (student's t-test). Individual data points represent biologic replicates, error bars indicate standard deviation.

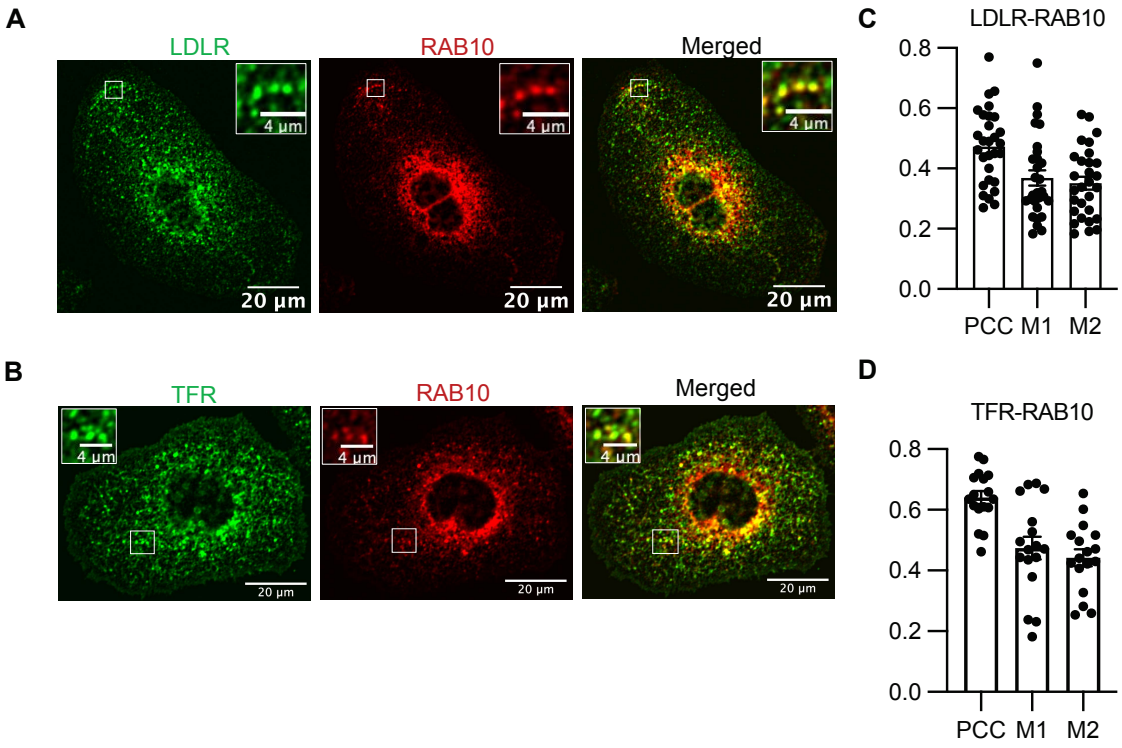

Figure 2.8 RAB10 colocalizes with LDLR and TFR.

Immunofluorescence of HuH7 cells (A, C) with Pearson's correlation coefficient and Mander's overlap coefficient (B, D) for colocalization between RAB10 and LDLR (A, B) or TFR (C, D). Individual data points represent individual cells imaged in three biologic replicates; error bars indicate standard deviation.

2.3 Discussion

Recycling of endocytosed membrane proteins to the cell surface plays an important role in maintaining the composition of the plasma membrane and the physiologic functions of the recycled proteins. Together with gene expression, protein secretion, and protein turnover, recycling regulates the steady state level of a given receptor protein on the cell surface. The initial endocytosis of integral membrane proteins shares similar features, with receptors often releasing their ligands in the acidic lumen of early endosomes. After complex dissociation, receptors may then recycle back to the plasma membrane, either directly or via the endocytic recycling compartment (ERC) and late recycling vesicles.

Rab GTPases have previously been reported to play broad roles in the regulation of vesicular trafficking. We recently identified the small GTPase RAB10 as a putative modifier of cellular LDL and transferrin uptake [5, 37, 38]. In the current report, we confirmed the discordant effects of RAB10 on LDL and transferrin cellular accumulation, with the former decreased and the latter

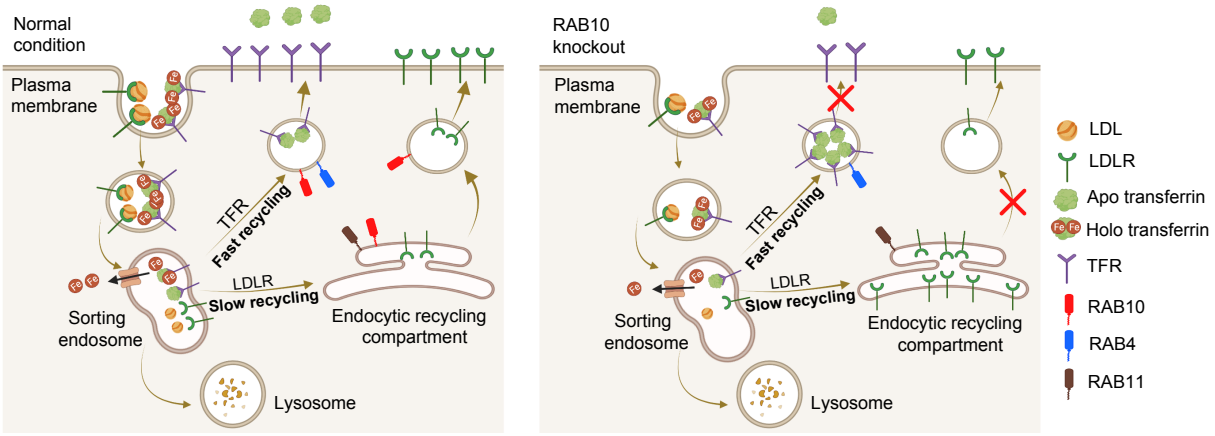

Figure 2.9 Differential effects of *RAB10* deletion on LDLR and TFR recycling.

(A) LDL bound LDLR and holo transferrin bound TFR undergo clathrin mediated endocytosis, upon which LDLR releases LDL and transferrin releases iron molecules within sorting endosome. LDLR is then transported via an endocytic recycling compartment (ERC) and recycled to the cell surface. The majority (80-90%) of apo transferrin bound TFR is recycled through a fast-recycling route to the cell surface. (B) Deletion of *RAB10* results in a defect in trafficking of both fast and slow recycling vesicles, leading to accumulation of LDLR in RAB11 positive ERC and TFR in RAB4 positive fast recycling vesicles, resulting in reduced cell surface LDLR and TFR. Despite both LDLR and TFR accumulating within recycling compartments, only transferrin, which remains in complex with TFR, also accumulates in *RAB10*-deleted cells, as LDL dissociates from LDLR and undergoes degradation within lysosomes.

increased upon RAB10 depletion (Fig. 1B-C). Unexpectedly, in contrast to the opposing effects of RAB10 depletion on LDL and transferrin uptake, we observed similar effects on their corresponding receptors, LDLR and TFR. This discrepancy was likely due to the different fates of the two ligands following uptake, with LDL undergoing dissociation from LDLR while transferrin remains in complex with TFR during recycling until its release extracellularly. This process is summarized schematically in Figure 7.

Several lines of evidence support a model in which RAB10 promotes the recycling of both LDLR and TFR. First, RAB10 depletion caused a decrease in the amount of both receptors on the cell surface without a corresponding decrease in gene expression (Fig. 2). Second, RAB10

depletion also caused an intracellular accumulation of both receptors in recycling organelles consistent with a delay in their plasma membrane recycling (Fig. 4H-I, Fig. 5G-H). Third, a subpopulation of RAB10 was found to colocalize with both receptors and with recycling endosomes. Fourth, the association of GTP locked RAB10 mutant with recycling endosomes was decreased, consistent with this active form accelerating the anterograde transport of cargo vesicles out of this compartment. Finally, kinetic experiments confirmed a delay in TFR recycling to the plasma membrane (Fig. 6D).

Previous studies have revealed heterogeneity in the recycling of different receptors, with some, including LDLR, transported along a RAB11-mediated slow recycling pathway involving the ERC, while others, including TFR, utilize both RAB11 and RAB4-mediated rapid recycling pathways . Our results implicate RAB10 in both pathways, as we observed LDLR accumulation in RAB11-positive punctae and TFR accumulation in RAB4-positive punctae upon RAB10 depletion. Small GTPases function as molecular switches, cycling between a GDP bound inactive state and GTP-bound active state that mediates recruitment of effector proteins to membranes. Intriguingly, GTP-bound RAB10 has previously been demonstrated to mediate the insulin-stimulated transport of GLUT4-containing vesicles to the plasma membrane via its recruitment of the exocyst membrane tethering complex [17]. Our prior screen of LDL uptake modifiers likewise identified several exocyst components including *EXOC1*, *EXOC2*, *EXOC3*, *EXOC4*, *EXOC7*, *EXOC8* that phenocopied *RAB10*, with depletion of either protein resulting in decreased LDL uptake and increased transferrin accumulation. Association of RAB10 with the exocyst complex has also been reported in renal epithelial cells [19]. Taken together, these findings suggest that RAB10 may promote the recycling of LDLR and TFR through the recruitment of the exocyst to recycling vesicles. The previously reported CRISPR screen for

modifiers of LDL uptake [13] also identified RABIF (Rab interacting factor), a guanine nucleotide exchange factor that stimulates GDP release from various Rab GTPases including RAB10, and which has also been shown to stabilize RAB10 [20]. This screen also identified STX4, a SNARE protein that facilitates docking and fusion of transport vesicle with the cell membrane and has been similarly implicated in the fusion of GLUT4 vesicles with the plasma membrane[17]. A recent study based on published proteomic data and CRISPR/Cas9 screens also identified a correlation between RAB10 and STX4[5]. Taken together, these findings suggest that RAB10, the exocyst, and STX4 may work together to coordinate the trafficking, tethering, and fusion of LDLR and TFR-containing recycling vesicles, similar to their role in GLUT4 vesicular trafficking.

RAB10 has also been implicated in diverse areas of membrane trafficking in different cell types, including formation of noncanonical macropinosome tubules in macrophages [39], vesicle transportation from early endosome to recycling endosome in C. elegans[40], and Golgi to plasma membrane transport in macrophages [12, 41-45]. Consistent with this wide range of functions, RAB10 has been localized to multiple subcellular compartments in different cell types including the endoplasmic reticulum, trans Golgi network, early endosomes, recycling endosomes, phagosomes, and primary cilia . We also observed significant subpopulations of RAB10 in several subcellular compartments. In further support of the breadth of cellular functions for RAB10, germline deletion of *RAB10* in mice results in embryonic lethality[1]. This latter observation limits the direct confirmation of our current findings in an in vivo mouse model and, together with our demonstration that multiple receptors depend on RAB10 for recycling, suggests that the potential for RAB10-mediated LDLR recycling as a therapeutic target is likely to be limited by substantial off-target effects.

2.4 Materials and Methods

Antibodies

Antibody	Supplier /ID	Experiment	Dilution
Anti LDLR	Proteintech; 10785-1-AP	Western blot	1:2000
Anti LDLR	Santa Cruz biotechnology; sc-18823(clone C7)	Immunofluorescence Endocytosis assay	1:400 1.25ul(0.25ug)/100ul
Anti LDLR	R & D system; FAB2148G Alexa488	Protein quantification by FACS	5ul/100ul(10^6 cells)
Anti TFR	Santa Cruz biotechnology; sc-65882/H68.4	western blot Immunofluorescence	1:1000 1:400
Anti TFR-FITC	Fisher/11-0719-42 (clone OKT9)	Protein quantification by FACS	5ul(0.125ug)/100ul(10^5-10^8 cells/100ul)
Anti Rab10	Abcam/ab237703	western blot Immunofluorescence	1:1000 1:400
Rabbit anti EEA1	Cell Signaling Technology, Inc./3288S(clone C45B10)	Immunofluorescence	1:100
Mouse anti EEA1	BD BIOSCIENCE /610456	Immunofluorescence	1:400
Rabbit Anti Rab11	Cell Signaling Technology /(clone D4F5) 5589S	Immunofluorescence	1:100
Mouse anti Rab11	Santa Cruz biotechnology /(clone D-3) sc-166523	Immunofluorescence	1:50
Rabbit anti LAMP1	Santa Cruz biotechnology /9091S	Immunofluorescence	1:100
Rabbit PDI	Cell Signaling Technology /3501S	Immunofluorescence	1:100
Mouse anti PDI	Thermo Scientific /MA3-019	Immunofluorescence	1:50
Rabbit TGN46	Abcam /ab50595	Immunofluorescence	1:100
Sheep anti Human TGN46	Bio-Rad/AHP500GT	Immunofluorescence	1:200
Rabbit anti GM130	Abcam/ab52649	Immunofluorescence	1:100
Rabbit anti Rab7(D95F2)	Cell Signaling Technology, Inc. / 9367T	Immunofluorescence	1:100
Donkey anti-Sheep IgG-Alexa Fluor 488	Thermo Scientific / A-11015	Immunofluorescence	1:500
Donkey anti Mouse IgG-Alexa Fluor 488	Thermo Scientific / A-21202	Immunofluorescence FACS	1:1000
Donkey anti Rabbit IgG-Alexa Fluor Plus 594	Fisher/ A32754	Immunofluorescence	1:500
β-Actin Antibody (C4)	Santa Cruz biotechnology /sc-47778	Western blot	1:1000
Anti mouse		Western blot	1:5000

Anti rabbit		Western blot	1:5000

Oligonucleotide sequences

RAB10 gRNA	TGATGGTGTGAAATCGCTCC
LDLR gRNA	AACAAGTTCAAGTGTCACAG
TFRC gRNA	CGGTAGACTTGTTTACCTGG
Non targeting gRNA	CGTGTGTGGGTAAACGGAAA

Plasmid, virus and cell culture

For CRISPR mediated gene knockouts, the sgRNA sequences were cloned into the CRISPR plasmid pLentiCRISPRv2(Addgene, MA, USA #52961) as previously described [47]. Virus particles were then prepared by co-transfection of cloned sgRNA together with pCMV-VSV-G (Addgene #8454) and (Addgene #12260) into HEK293T cells with Lipofectamine LTX (ThermoFisher). Media was replaced at 12 hr post transfection. Conditioned media containing virus were harvested at 48 hr post-transfection, centrifuged at 1000g for 10 mins, and the resulting supernatant stored at -80℃ for future use. To generate knockout cells, HuH7 cells were transduced with lentivirus carrying the corresponding sgRNA, selected for transduced cells with puromycin, and passaged for two weeks to allow time for target site mutagenesis and turnover of wild type protein. *RAB10* knockout clonal cell lines were derived by diluting cell suspensions into 96 well plates. Wells containing a single colony of growth were then expanded. Selected clonal cell lines were analyzed by immunofluorescence and immunoblotting. RAB10 expression constructs were generated by cloning CRISPR resistant cDNA sequences and a blasticidin resistance cassette into the lentiviral expression vector LeGO-iC2(Addgene, 27345) using GIBSON assembly mix purchased from NEB (NEBuilder HiFi DNA Assembly). HEK293T and HuH7 cells were cultured in Dulbecco's modified Eagle's medium (DMEM) supplemented with 10% fetal bovine serum, and 100 U/ml penicillin, 100 mg/ml streptomycin (Thermo Scientific) at 37℃ in a 5% CO2-conditioned, humidified incubator.

LDL and transferrin uptake assay

Cells were seeded in 6 well plates to achieve ~70%-80% confluence on the day of analysis. For uptake assays, cells were washed with serum free DMEM and then incubated in DMEM containing either 4 µg/ml DyLight550-conjugated LDL (Cayman Chemical) or 5 µg/ml Alexa Fluor 555 conjugated transferrin (ThermoFisher Scientific) at 37˚C for 1 hour or 30 mins, respectively. Cells were harvested with TrypLE express (ThermoFisher Scientific), washed with ice cold PBS, resuspended in 150ul of ice-cold PBS, and analyzed with a Bio-Rad Ze5 flow cytometer. Data analysis was performed with FlowJo (FlowJo).

Western blot

Cells were cultured at 37˚C in 10 cm dish until 70-80% confluent. Cells collected with trypLE express were washed in PBS, and then lysed in RIPA lysis and extraction buffer (Thermo Scientific) containing complete protease inhibitor cocktail (Roche). After brief sonication, lysed cell suspensions were rotated at 4˚C for 1 hr for protein extraction followed by centrifugation at 15000g. Protein concentration was determined with the Bio-Rad DC assay kit (Bio-Rad, # 500-0111) and SDS-PAGE was performed using NuPAGE™ 4 to 12%, Bis-Tris, mini protein gels (ThermoFisher Scientific # NP0321BOX) according to manufacturer's instruction. Western blot transfer was done into nitrocellulose membrane (Thermo scientific #IB23002) using the iBlot 2 Dry Blotting System (Thermo Scientific).

Flow cytometry

HuH7 cells cultured in 6 well plates were prepared for analysis at 70-80% confluence. For surface staining, collected cells were washed three times with ice cold blocking buffer (PBS, 2% FBS), resuspended at approximately 106 cells in 1 mL blocking buffer and incubated for 30 mins with end-over-end rotation at 4˚C. After centrifugation at 400g for 5 mins, cells were

resuspended in fluorescently labelled LDLR antibody or TFR antibody diluted in 100 µl blocking buffer and incubated for 1 hr in the dark at 4oC. Cells were then washed 3 times with ice cold PBS, resuspended in 150 µl cold PBS for final analysis by flow cytometry (Bio-Rad ZE5). For quantification of total cellular LDLR or TFR, harvested cells were fixed with 2% PFA for 10 minutes followed by PBS wash and permeabilization with 500 µl of 0.5% saponin in PBS before proceeding with staining for LDLR and TFR.

Immunofluorescence and confocal microscopy

Cells cultured on poly-D-lysine coated glass coverslips (Electron Microscopy Sciences, #72294-11) were fixed in 2% paraformaldehyde for 15 mins in the dark at room temperature. After washing three times with PBS, cells were then permeabilized with 0.1% saponin in PBS for 5 mins, incubated for 1 hr in blocking buffer (PBS with 4% FBS and 40mM glycine), stained with primary antibody at indicated dilutions in PBS with 4% FBS for 1 hr, washed with PBS three times, stained with secondary antibody at indicated dilutions in PBS with 4% FBS for 1 hr, and washed with PBS three times. Coverslips were mounted on glass slides with Prolong Diamond antifade mounting reagent (Invitrogen). Images were acquired with a NIKON A1 standard sensitivity (SS) confocal microscope with 60X (NA51.4) oil objective. Colocalization quantification was done using the open-source Fiji (Image J) software. Mander's coefficient and Pearson's coefficient were calculated using JACop in Image J. A total of 10-30 cells from two to three biological replicates were analyzed. For all quantitative analysis, the observer was blinded to cell genotype.

Endocytosis assay

An assay for transferrin receptor endocytosis was adapted from previous reports . Briefly, cells grown in 10 cm dishes were serum starved in DMEM for 30 mins, harvested in tryPLE Express

(ThermoFisher Scientific), washed in ice cold DMEM, incubated with Alexa Fluor 555-conjugated transferrin in DMEM at 4℃, and rotated for 1 hr. Unbound excess transferrin was removed by washing cells with PBS and surface bound transferrin internalization was induced by incubating cells in prewarmed complete culture medium at 37˚C for various time points. At each time point, an excess of ice-cold PBS was added to a sample to stop internalization, cells were collected by centrifugation, and surface bound transferrin was removed with ice-cold acid wash buffer (0.1 M glycine and 150 mM NaCl, pH 3) followed by three PBS washes. Cells were resuspended in ice-cold PBS and analyzed by flow cytometry on a BioRad ZE5. 10000-15000 cells were analyzed for each time point.

An assay for LDLR endocytosis was adapted from previous reports . Briefly, after PBS wash, cells were incubated in blocking buffer (2% FBS in PBS) for 30 mins at 4˚C. Surface LDLR was then stained with LDLR antibody for 1 hr at 4℃ and cells were washed with PBS to remove excess antibody. Cells were then incubated with prewarmed media at 37˚C for the indicated duration of time. At each time point, ice-cold blocking buffer was added to the sample, cells were collected by centrifugation, and the remaining surface-exposed LDLR antibody was labeled by incubation with fluorescent secondary antibody for 1 hour at 4˚C followed by three PBS washes. Cells were resuspended in ice-cold PBS. Analysis was performed by flow cytometry on a BioRad ZE5, with 10000-15000 cells analyzed for each time point.

Recycling assay

An assay for transferrin recycling was adapted from a previous report [1]. Briefly, cells were serum starved for 30 min in DMEM, incubated with Alexa Fluor 555 transferrin for 30 minutes at 37˚C, and washed with ice-cold PBS. Surface-bound transferrin was then removed by cold acid wash (0.1 M glycine and 150 mM NaCl, pH 3) followed by a PBS wash. Cell samples were

resuspended in pre-warmed media at 37˚C for the indicated times. A second acid wash followed by PBS wash was done after which samples were analyzed by flow cytometry.

2.5 References

1. Brown, M.S. and J.L. Goldstein, Regulation of the activity of the low density lipoprotein receptor in human fibroblasts. Cell, 1975. 6(3): p. 307-16.
2. Ciechanover, A., et al., Kinetics of internalization and recycling of transferrin and the transferrin receptor in a human hepatoma cell line. Effect of lysosomotropic agents. J Biol Chem, 1983. 258(16): p. 9681-9.
3. Dautry-Varsat, A., Receptor-mediated endocytosis: the intracellular journey of transferrin and its receptor. Biochimie, 1986. 68(3): p. 375-81.
4. Mayle, K.M., A.M. Le, and D.T. Kamei, The intracellular trafficking pathway of transferrin. Biochim Biophys Acta, 2012. 1820(3): p. 264-81.
5. Emmer, B.T., et al., Genome-scale CRISPR screening for modifiers of cellular LDL uptake. PLoS Genet, 2021. 17(1): p. e1009285.
6. Chua, C.E.L. and B.L. Tang, Rab 10-a traffic controller in multiple cellular pathways and locations. J Cell Physiol, 2018. 233(9): p. 6483-6494.
7. English, A.R. and G.K. Voeltz, Rab10 GTPase regulates ER dynamics and morphology. Nat Cell Biol, 2013. 15(2): p. 169-78.
8. Seabra, M.C., E.H. Mules, and A.N. Hume, Rab GTPases, intracellular traffic and disease. Trends Mol Med, 2002. 8(1): p. 23-30.
9. Zerial, M. and H. McBride, Rab proteins as membrane organizers. Nat Rev Mol Cell Biol, 2001. 2(2): p. 107-17.
10. Goldstein, J.L., R.G. Anderson, and M.S. Brown, Receptor-mediated endocytosis and the cellular uptake of low density lipoprotein. Ciba Found Symp, 1982(92): p. 77-95.
11. Brown, M.S., J. Herz, and J.L. Goldstein, LDL-receptor structure. Calcium cages, acid baths and recycling receptors. Nature, 1997. 388(6643): p. 629-30.
12. Brown, M.S. and J.L. Goldstein, A receptor-mediated pathway for cholesterol homeostasis. Science, 1986. 232(4746): p. 34-47.
13. Chen, C.C., et al., RAB-10 is required for endocytic recycling in the Caenorhabditis elegans intestine. Mol Biol Cell, 2006. 17(3): p. 1286-97.
14. Wang, D., et al., Ras-related protein Rab10 facilitates TLR4 signaling by promoting replenishment of TLR4 onto the plasma membrane. Proc Natl Acad Sci U S A, 2010. 107(31): p. 13806-11.
15. Sano, H., et al., Rab10, a target of the AS160 Rab GAP, is required for insulin-stimulated translocation of GLUT4 to the adipocyte plasma membrane. Cell Metab, 2007. 5(4): p. 293-303.
16. Schuck, S., et al., Rab10 is involved in basolateral transport in polarized Madin-Darby canine kidney cells. Traffic, 2007. 8(1): p. 47-60.
17. Allaire, P.D., et al., The Connecdenn DENN domain: a GEF for Rab35 mediating cargo-specific exit from early endosomes. Mol Cell, 2010. 37(3): p. 370-82.
18. Kouranti, I., et al., Rab35 regulates an endocytic recycling pathway essential for the terminal steps of cytokinesis. Curr Biol, 2006. 16(17): p. 1719-25.

19. Beisiegel, U., et al., Monoclonal antibodies to the low density lipoprotein receptor as probes for study of receptor-mediated endocytosis and the genetics of familial hypercholesterolemia. J Biol Chem, 1981. 256(22): p. 11923-31.
20. Maurer, M.E. and J.A. Cooper, The adaptor protein Dab2 sorts LDL receptors into coated pits independently of AP-2 and ARH. J Cell Sci, 2006. 119(Pt 20): p. 4235-46.
21. Du, L. and S.R. Post, Macrophage colony-stimulating factor differentially regulates low density lipoprotein and transferrin receptors. J Lipid Res, 2004. 45(9): p. 1733-40.
22. Maxfield, F.R. and T.E. McGraw, Endocytic recycling. Nat Rev Mol Cell Biol, 2004. 5(2): p. 121-32.
23. Ghosh, R.N., D.L. Gelman, and F.R. Maxfield, Quantification of low density lipoprotein and transferrin endocytic sorting HEp2 cells using confocal microscopy. J Cell Sci, 1994. 107 (Pt 8): p. 2177-89.
24. Boucrot, E. and T. Kirchhausen, Endosomal recycling controls plasma membrane area during mitosis. Proc Natl Acad Sci U S A, 2007. 104(19): p. 7939-44.
25. Grant, B.D. and J.G. Donaldson, Pathways and mechanisms of endocytic recycling. Nat Rev Mol Cell Biol, 2009. 10(9): p. 597-608.
26. O'Sullivan, M.J. and A.J. Lindsay, The Endosomal Recycling Pathway-At the Crossroads of the Cell. Int J Mol Sci, 2020. 21(17).
27. Mayor, S., J.F. Presley, and F.R. Maxfield, Sorting of membrane components from endosomes and subsequent recycling to the cell surface occurs by a bulk flow process. J Cell Biol, 1993. 121(6): p. 1257-69.
28. Sheff, D.R., et al., The receptor recycling pathway contains two distinct populations of early endosomes with different sorting functions. J Cell Biol, 1999. 145(1): p. 123-39.
29. Sano, H., et al., A potential link between insulin signaling and GLUT4 translocation: Association of Rab10-GTP with the exocyst subunit Exoc6/6b. Biochem Biophys Res Commun, 2015. 465(3): p. 601-5.
30. Babbey, C.M., R.L. Bacallao, and K.W. Dunn, Rab10 associates with primary cilia and the exocyst complex in renal epithelial cells. Am J Physiol Renal Physiol, 2010. 299(3): p. F495-506.
31. Gulbranson, D.R., et al., RABIF/MSS4 is a Rab-stabilizing holdase chaperone required for GLUT4 exocytosis. Proc Natl Acad Sci U S A, 2017. 114(39): p. E8224-e8233.
32. Leto, D. and A.R. Saltiel, Regulation of glucose transport by insulin: traffic control of GLUT4. Nat Rev Mol Cell Biol, 2012. 13(6): p. 383-96.
33. Clague, M.J. and S. Urbé, Data mining for traffic information. Traffic, 2020. 21(1): p. 162-168.
34. Kawai, K., et al., Rab10-Positive Tubular Structures Represent a Novel Endocytic Pathway That Diverges From Canonical Macropinocytosis in RAW264 Macrophages. Front Immunol, 2021. 12: p. 649600.
35. Lerner, D.W., et al., A Rab10-dependent mechanism for polarized basement membrane secretion during organ morphogenesis. Dev Cell, 2013. 24(2): p. 159-68.
36. Etoh, K. and M. Fukuda, Rab10 regulates tubular endosome formation through KIF13A and KIF13B motors. J Cell Sci, 2019. 132(5).
37. Leaf, D.S. and L.D. Blum, Analysis of rab10 localization in sea urchin embryonic cells by three-dimensional reconstruction. Exp Cell Res, 1998. 243(1): p. 39-49.
38. Lv, P., et al., Targeted disruption of Rab10 causes early embryonic lethality. Protein Cell, 2015. 6(6): p. 463-467.

39. Alonso, R., et al., PCSK9 and lipoprotein (a) levels are two predictors of coronary artery calcification in asymptomatic patients with familial hypercholesterolemia. Atherosclerosis, 2016. 254: p. 249-253.
40. Ahotupa, M., Oxidized lipoprotein lipids and atherosclerosis. Free Radic Res, 2017. 51(4): p. 439-447.
41. Brown, M.S. and J.L. Goldstein, The SREBP pathway: regulation of cholesterol metabolism by proteolysis of a membrane-bound transcription factor. Cell, 1997. 89(3): p. 331-40.
42. Zelcer, N., et al., LXR regulates cholesterol uptake through Idol-dependent ubiquitination of the LDL receptor. Science, 2009. 325(5936): p. 100-4.
43. Ivanova, E.A., et al., Small Dense Low-Density Lipoprotein as Biomarker for Atherosclerotic Diseases. Oxid Med Cell Longev, 2017. 2017: p. 1273042.
44. Fedoseienko, A., et al., The COMMD Family Regulates Plasma LDL Levels and Attenuates Atherosclerosis Through Stabilizing the CCC Complex in Endosomal LDLR Trafficking. Circ Res, 2018. 122(12): p. 1648-1660.
45. Ference, B.A., et al., Low-density lipoproteins cause atherosclerotic cardiovascular disease. 1. Evidence from genetic, epidemiologic, and clinical studies. A consensus statement from the European Atherosclerosis Society Consensus Panel. Eur Heart J, 2017. 38(32): p. 2459-2472.
46. Brown, M.S. and J.L. Goldstein, Receptor-mediated endocytosis: insights from the lipoprotein receptor system. Proc Natl Acad Sci U S A, 1979. 76(7): p. 3330-7.
47. Davis, C.G., et al., Acid-dependent ligand dissociation and recycling of LDL receptor mediated by growth factor homology region. Nature, 1987. 326(6115): p. 760-5.
48. Horton, J.D., J.C. Cohen, and H.H. Hobbs, Molecular biology of PCSK9: its role in LDL metabolism. Trends Biochem Sci, 2007. 32(2): p. 71-7.
49. Bartuzi, P., et al., CCC- and WASH-mediated endosomal sorting of LDLR is required for normal clearance of circulating LDL. Nat Commun, 2016. 7: p. 10961.

Chapter 3 Genome-Wide CRISPR Screen for Regulators of Lp(a) Uptake by HuH7 Cells

Abstract

Despite its importance in the pathogenesis of atherosclerosis and calcific aortic valve stenosis, the molecular regulation of lipoprotein(a) (Lp(a)) homeostasis remains poorly understood. In particular, it remains uncertain which of several proposed Lp(a) receptors is responsible for hepatic Lp(a) clearance. We now report our development and execution of a whole-genome CRISPR screen for modifiers of Lp(a) uptake in liver-derived HuH7 cells. We first optimized a strategy for Lp(a) fluorescent labeling and fluorescent uptake, which we then applied to pooled libraries of CRISPR-edited cells to isolate the subpopulations with reduced or enhanced Lp(a) uptake. The top positive Lp(a) uptake regulator identified by this screen was LDLR (low density lipoprotein receptor) (FDR<5%), and the top negative regulator was MYLIP (FDR<5%), which encodes the LDLR-specific ubiquitin ligase IDOL. We also identified other known regulators of LDLR, including SCAP, MBTPS2, and other genes we had previously identified in a similar screen for LDL uptake modifiers. CRISPR guide RNAs targeting other previously proposed Lp(a) receptors exhibited no effect on Lp(a) uptake, and no specific enrichment was observed for other functional annotations or known protein-protein interactions. Taken together, these results are consistent with a model in which Lp(a) uptake by hepatocytes is primarily mediated by the LDL receptor.

3.1 Introduction

Lipoprotein(a) (Lp(a)) is a highly atherogenic, proinflammatory and prothrombotic cholesterol- carrying particle. Increased levels of Lp(a) in the bloodstream confer an increased risk of cardiovascular diseases including myocardial infarction, peripheral artery disease, calcific aortic valve stenosis, and stroke [2-9]. Structurally, Lp(a) consists of an LDL (low density lipoprotein) core covalently bound to a highly glycosylated plasminogen-like protein called apolipoprotein(a), or apo(a), encoded by the *LPA* gene [10]. The concentration of Lp(a) in the bloodstream is influenced by the allelic heterogeneity of *LPA* [11, 12]. Apo(a) contains an inactive serine protease domain, one kringle V (KV) domain and 10 different types of kringle IV (KIV) domains. Kringle IV type 2 (KIV2) is present in humans with a highly variable number of repeats, ranging from 1 to >40 copies. The number of KIV2 repeats in a given *LPA* allele is inversely related to the corresponding steady state Lp(a) plasma concentration, with functional studies suggesting that smaller apo(a) isoforms are secreted more efficiently by hepatocytes than the high molecular weight isoforms[13]. Several common genetic variants identified in the *LPA* gene are associated with Lp(a) concentrations, potentially due to different rates of apo(a) biosynthesis[4, 14, 15].

Although physiologic variation in plasma Lp(a) has been mainly attributed to differences in Lp(a) synthesis and secretion, the steady state level of Lp(a) is also dependent on its rate of clearance. Lp(a) clearance from circulation occurs primarily in the liver but the molecular basis for this remains unclear[16]. A specific receptor has not been definitively identified due to lack of consensus between different in vivo and in vitro investigations suggesting a range of different receptors for cellular endocytosis of Lp(a). Due to the structural similarities of Lp(a) and LDL, a potential role for the LDL receptor (LDLR) in Lp(a) clearance has been extensively studied in

vitro and in vivo with inconsistent results[17-19]. Several other candidate receptors including VLDLR, LRP, megalin, TLR, SR-B1, ASGPR1, galectin-1, PlgRKT and sortilin have also been tested for a role in Lp(a) uptake, with inconsistent or conflicting results [20, 21]. To date, no high-throughput functional approach has been applied to systematically interrogate the relative contributions of all potential Lp(a) receptors to Lp(a) hepatocellular uptake. We now report our development and execution of a genome-scale CRISPR screen for modifiers of Lp(a) uptake in HuH7, a liver-derived cell line that closely matches primary human hepatocytes and has been previously used as a model system to study LDL and Lp(a) metabolism. This forward genetic tool enabled us to systematically interrogate nearly all coding genes and test all possible receptors including previously suggested Lp(a) receptors and any potential regulators of these receptors. Our findings support a model in which LDLR plays a dominant role in hepatic Lp(a) clearance.

3.2 Results

Fluorescent labeling of purified Lp(a) particles.

To facilitate FACS-based screening of CRISPR-edited cells according to their capacity for Lp(a) endocytosis, we first developed a method for Lp(a) fluorescent labeling. Using commercial Lp(a) preparations derived from human plasma donors, we tested different reagents for fluorescent labeling of Lp(a) particles. Our initial attempts with NHS ester-based labeling by FITC, or pHrodo-Red and with lipid labeling by DiI (1,1'-Dioctadecyl-3,3,3',3'-Tetramethylindocarbocyanine Perchlorate) were complicated by significant lipoprotein precipitation (Figure 3.1A, B). Labeling with an STP-ester amine reactive dye, pHrodo-iFL-Red, which is more hydrophilic than conventional NHS ester dyes[22], avoided this precipitation, with successful labeling confirmed by SDS-PAGE gel electrophoresis and in-gel scanning of

fluorescent signal of Lp(a) conjugated dye (Figure 3.1C). Silver staining demonstrated the efficient recovery of lipoprotein with densitometric analysis showing approximately 85% recovered after labeling (Figure 3.1D). In parallel as a control, we also labeled LDL to assess efficiency of the labeling strategy (Figure 3.1F, G). During labeling optimization with varying dye to protein molar ratios, we observed precipitation of Lp(a) with increased concentration of dye, whereas LDL was stable with no precipitation. This suggests that the apo(a) component confers increased hydrophobicity and structural complexity to Lp(a), rendering Lp(a) particles less stable to a further increase in hydrophobicity by conjugation of a hydrophobic dye. To assess the potential LDL contamination of the Lp(a) preparation, we also analyzed both unlabeled and labeled Lp(a) preparations under non-reducing conditions, with the expectation that ApoB associated with LDL would have an unchanged electrophoretic mobility while ApoB associated with Lp(a) would migrate at a higher molecular weight (MW) consistent with its disulfide linkage to apo(a). Silver staining indeed revealed a dominant band at a MW consistent with an apo(a)/ApoB heterodimer, though a faint band with a MW band consistent with ApoB monomer

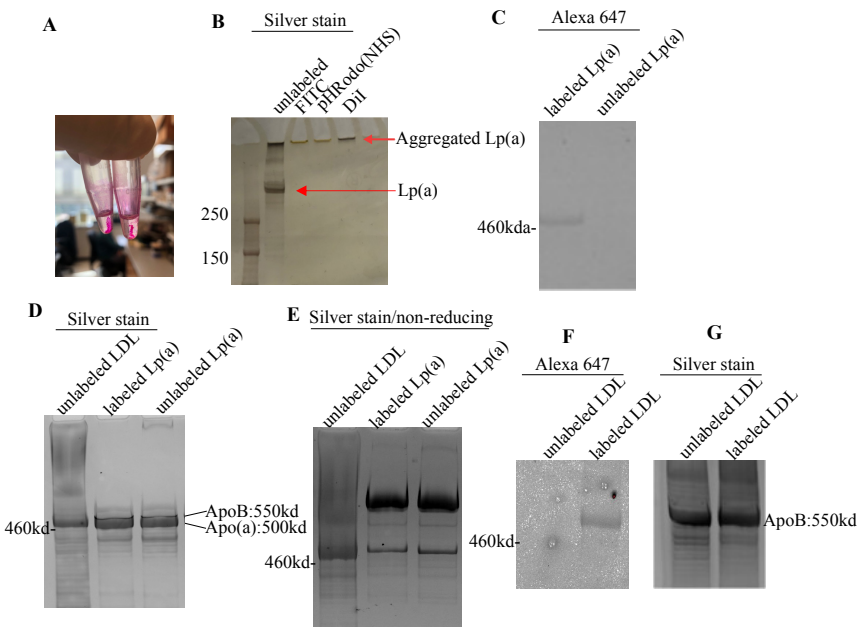

Figure 3.1 Fluorescent labeling of lipoprotein preparations.

Precipitation of Lp(a) samples during fluorescent labeling with DiI(A, B), FITC and pHrodo(NHS) (B). Fluorescent labeling of Lp(a) (C-E) and LDL (F-G) was evaluated by fluorescence scanning (C, F) and silver staining (D, E, G) of labeled and unlabeled lipoprotein preparations separated by SDS-PAGE under reducing conditions (C-D, F-G) or nonreducing (E) conditions.

(500 KD) remained visible, likely reflecting a minor amount of contaminating LDL (Figure 3.1E).

Development of a flow cytometry assay for quantification of fluorescent Lp(a) uptake.

We next analyzed the uptake of fluorescently labeled Lp(a) by HuH7 cells. Following a 2 hour incubation with 10 μg/mL of fluorescently conjugated Lp(a) in serum-free media, HuH7 cells exhibited a readily detectable fluorescent signal by flow cytometry (Figure 3.2A). Consistent with HuH7 Lp(a) uptake occurring via receptor-mediated endocytosis, co-incubation with an excess of unlabeled Lp(a) led to a dose-dependent reduction in the uptake of fluorescent Lp(a), albeit to a lesser degree than observed for LDL uptake inhibition by unlabeled LDL (Figure 3.2A, B). Together these findings demonstrate that fluorescent Lp(a) uptake is readily detectible in HuH7 cells.

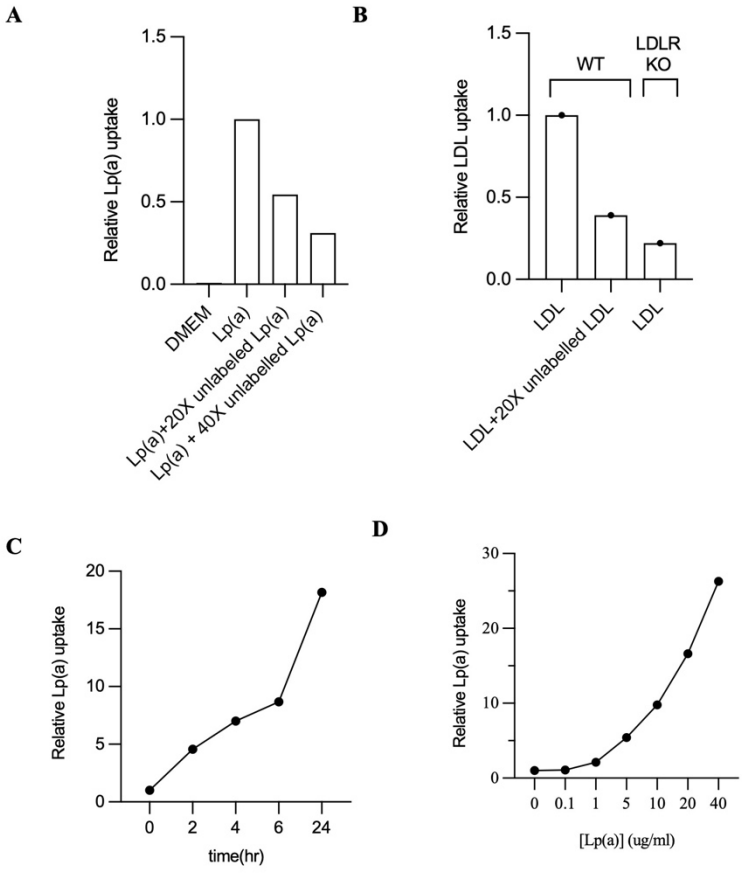

Figure 3.2 Assay development for fluorescent Lp(a) uptake.

(A) HuH7 cells were treated with DMEM (control) or labeled Lp(a) in the absence or presence of 20-fold or 40-fold molar excess of unlabeled Lp(a). Lp(a) uptake was measured by flow cytometry. (B) LDL uptake by WT and LDLR knockout HuH7 cells. WT cells were incubated with labeled LDL in the presence or absence of excess unlabeled LDL. LDLR KO cells were only treated with labeled LDL. (C-D) Time and dose curve for fluorescent Lp(a) uptake by WT HuH7 cells. Cells were treated with either 10 μg/mL Lp(a) for different lengths of time (C) or with different doses of Lp(a) for 2 hours (D). Uptake of Lp(a) was measured by FACS.

To further define the kinetics of Lp(a) uptake we incubated HuH7 cells with 10 μg/mL fluorescent Lp(a) for times ranging from 1 hour to 24 hours (Figure 3.2C). Next, we examined the dose-dependency of Lp(a) uptake by HuH7 cells by incubating these cells with a range of labeled Lp(a) concentrations for 2 hrs (Figure 3.2D). We observed steady increases in the magnitude of fluorescence with increased duration of incubation and with increased Lp(a) concentration, without reaching a plateau in either experiment.

Genome-scale CRISPR screen for Lp(a) uptake modifiers

Informed by the results of our fluorescent Lp(a) uptake analysis above, we next designed a genome-scale CRISPR screen to identify genes whose perturbation altered fluorescent Lp(a) uptake (Figure 3.3A). For each of 3 independent biological replicates, we transduced ~55 million cells at >400X coverage with the pooled GeCKOv2 library delivering Cas9 with each of 123,411 gRNAs, including 6 gRNA for nearly all known protein-coding genes in the genome[23]. We then selected for transduced cells and passaged cells for 14 days to allow for target gene disruption and turnover of residual protein. We then incubated pools of CRISPR-edited cells with 20 ug/ml fluorescent Lp(a) for 2 hours and used flow cytometry to isolate subpopulations with the top 10% and bottom 10% of fluorescent Lp(a) uptake. We then performed massively parallel sequencing to quantify the abundance of each gRNA in each subpopulation for each replicate.

We next identified gRNAs with significant enrichment in either Lp(a)high or Lp(a)low cells, consistent with disruption of their corresponding target gene conferring an increase or decrease, respectively, in Lp(a) uptake. Overall, we identified several genes whose disruption

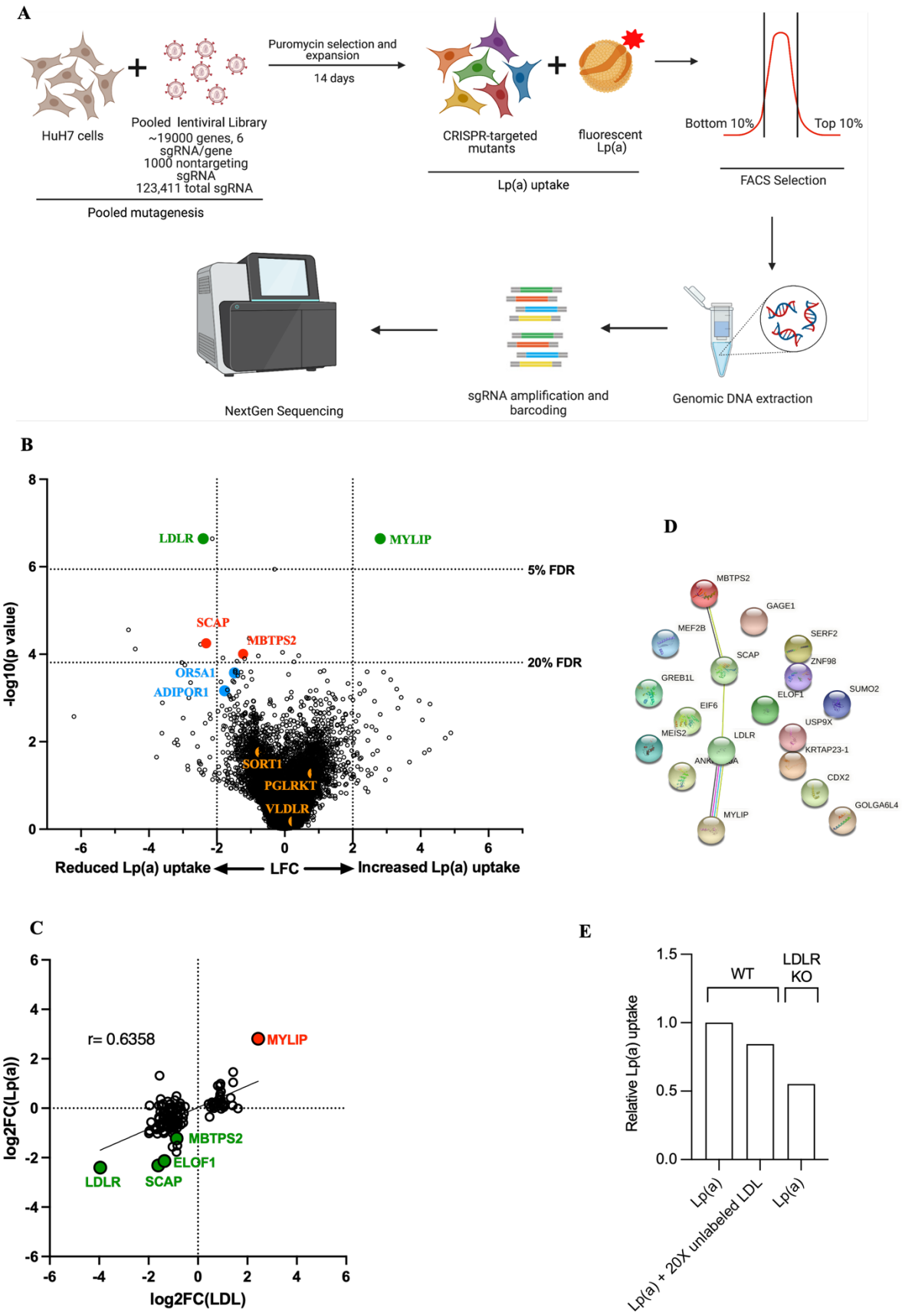

was associated with a significant increase or decrease in Lp(a) uptake (Figure 3.3B). Strikingly,

Figure 3.3 CRISPR screens for Lp(a) uptake modifiers in HuH7.

(A) Schematic for genome-scale CRISPR screen. HuH7 WT cells were mutagenized with the pooled GeCKOv2 lentivirus library containing 6 gRNAs for each protein coding gene. After transduction and puromycin selection, cells were incubated with fluorescent Lp(a). Populations of gene edited cells with increased or decreased Lp(a) uptake efficiency were sorted into separate pools. Genomic DNA was harvested from each sorted population and sgRNAs in each population were quantified by massively parallel DNA sequencing. (B) Volcano plot of MAGeCK gene-level FDR (negative log) and log2 fold-change for each gene tested in the whole genome CRISPR library in HuH7 cells. Genes with FDR <5% and log2 fold-change >2 are highlighted in green. Genes with known function in LDLR regulation are displayed in red. Other hits identified in the screen with a known transmembrane domain are highlighted in blue and genes previously predicted to regulate Lp(a) uptake but not identified in the CRISPR screen are highlighted in orange. (C) Correlation of log2 fold-change between the hits identified in previous LDL uptake screen[1] and the current Lp(a) uptake screen in HuH7 cells. Genes identified in both screens are highlighted and annotated. (D) Protein-protein interaction network of genes identified in our Lp(a) uptake screen with FDR<20%. (E) Wild type (WT) HuH7 cells were treated with labeled Lp(a) in the absence or presence of 20-fold molar excess of unlabeled LDL. And LDLR knockout cells were treated only with labeled Lp(a). Cellular fluorescence was measured by flow cytometry.

among the top hits of the screen were several genes with well-established roles in LDL uptake. These included the top-ranked positive regulator, LDLR(FDR<5%), and the top-ranked negative regulator, MYLIP(FDR<5%), encoding the LDLR-specific ubiquitin ligase IDOL [24]. Other identified genes with a known role in LDL uptake included SCAP and MBTPS2 (Figure 3.3B). Similarly, a systematic comparison of gRNA enrichment between this Lp(a) uptake screen and our previous screen for LDL uptake modifiers[25] revealed a high degree of correlation between the two independent screens (Fig 3.3C). Among the other screen hits, only OR5A1 and ADIPOR1[26] are known to contain a transmembrane domain and localize to the cell surface. Of note, we did not identify a significant effect for disruption of any other previously proposed lipoprotein(a) receptors, including PLGRKT, VLDLR, SORT1 (Figure 3.3B). Analysis of screen hits for functional annotations and known gene networks likewise revealed only the known LDLR regulatory network. An unbiased analysis confirmed a protein-protein network involving LDLR, SCAP, MBTPS2, and MYLIP (FDR<20%), with no other significantly enriched gene networks (Figure 3.3D). In follow up experiments we confirmed that a molar excess of unlabeled LDL also reduced fluorescent Lp(a) endocytosis, suggesting that Lp(a) uptake occurs via a process common to both Lp(a) and LDL particles (Figure 3.3E). Similarly, uptake by LDLR knockout cells also showed a reduction in Lp(a) uptake, though the relative decrease was less than that observed for LDL uptake (Figure 3.3E, 3.2B).

3.3 Discussion

Given the structural similarities between LDL and Lp(a), the LDL receptor has long been considered as a candidate receptor for hepatic Lp(a) clearance. However, studies of the role of LDLR in Lp(a) clearance have yielded mixed results. In support of LDLR functioning as an Lp(a) clearance receptor, patients with familial hypercholesterolemia (FH) caused by partial or total loss of function mutations in LDLR have been reported to exhibit elevated circulating Lp(a) levels [17, 27, 28]. A gene-dosage effect has also been demonstrated, wherein patients with hypomorphic LDLR alleles exhibit less pronounced elevation of Lp(a) compared to those with complete loss-of-function mutations, and homozygous FH patients exhibit higher Lp(a) levels than heterozygous FH patients [17, 29]. In contrast, other studies have demonstrated no difference in circulating Lp(a) levels [30] or in the clearance of radiolabeled Lp(a) [31] in patients with FH. As noted in the introduction, common variation at the *LPA* locus itself exerts a strong confounding effect on Lp(a) levels, and these negative studies did not account for *LPA* genotype. On the other hand one positive study that matched FH and non-FH patients by apo(a) isoform indeed found that LDLR genetic deficiency was associated with a significant increase in Lp(a) levels across *LPA* genotypes. [29].

Two major classes of LDL-lowering medications - statins and PCSK9 inhibitors - have been reported to exert inconsistent effects on Lp(a) levels, despite both drug classes causing an increase in LDLR activity. Several randomized clinical trials have demonstrated no change in Lp(a) levels with statin treatment[32], whereas PCSK9 inhibitors have been found to produce a consistent 20-30% decrease in circulating Lp(a)[30, 33, 34]. The basis for this discrepancy is not clear but may be related to secondary effects, with statin treatment also leading to upregulation of PCKS9 [35] while PCSK9 inhibitors also affect Lp(a) synthesis[36].

Several studies have identified other candidate receptors for Lp(a), with varying levels of evidence, using different cell types and varying methods of gene perturbation[21, 37, 38]. It has also been proposed that physiologic Lp(a) clearance may be mediated not by a single receptor but by multiple receptors with additive effects[20].

The application of genome-wide CRISPR screening reported here systematically interrogated all potential Lp(a) receptors, with our findings suggesting that Lp(a) uptake in HuH7 cells is primarily mediated by the LDL receptor, with no significant enrichment observed for gRNAs targeting any of the other proposed Lp(a) receptors. Though we cannot exclude contributions of other genes or receptors to the regulation of cellular Lp(a) uptake, our data suggest that the contribution of any such alternative receptors to Lp(a) uptake in HuH7 cells is likely small in comparison to LDLR. Our results are also consistent with previous reports in HuH7 cells and another liver derived cell line, HepG2 [39, 40].

An important caveat to our approach is that it would likely fail to detect genes that are essential to cell viability or proliferation, as the corresponding edited cells would be progressively depleted during cell passaging. The CRISPR screening approach is also limited in its ability to detect functionally overlapping genes- i.e., knockout of a gene with a closely related paralog that can also mediate Lp(a) uptake could be missed if activity of one paralog compensated for loss of the other. Moreover, although the gRNAs present in the GECKOv2 library typically exhibit high rates of activity[23], it is possible that the gRNAs for a putative Lp(a) receptor may have inadequate activity, precluding their detection in the screen and leading to a false negative result.

Finally, it should be noted that our Lp(a) preparations were purified from human plasma and may contain co-purified LDL. Although our detection of ApoB protein not incorporated in ApoB-apo(a) complexes under nonreducing conditions does suggest some degree of LDL

contamination, the relative abundance of these putative LDL particles was ~20-fold less than Lp(a). Nonetheless, we cannot exclude the possibility that small amounts of contaminating labeled LDL may have contributed to the enrichment of gRNAs targeting LDLR modifiers in our screen. Overall, our findings demonstrate the power of high-throughput CRISPR screening to identify functional modifiers of lipoprotein metabolism and support the role of the LDL receptor in hepatic Lp(a) clearance.

3.4 Materials and Methods

Fluorescent labelling of Lp(a) and LDL

Human plasma derived Lp(a) and LDL (Athens Research and Technology, Georgia, USA #12-16-12160, # 12-16-120412-TC) were labelled with amine-reactive pHrodo- iFL Red STP ester dye (ThermoFisher, # P36014) at 1:28 molar ratio of protein to dye for 15 minutes in the dark at room temperature. Unconjugated free dye was removed from each sample by extensive dialysis against cold phosphate buffered saline. Labelled and unlabeled Lp(a) and LDL samples were prepared for SDS-PAGE by diluting in NuPAGE LDS sample buffer (ThermoFisher Scientific # NP0007) in presence or absence of reducing agent (DTT), and then heating at 70°C for 10 minutes. Gel electrophoresis was run using NuPAGE 3-8% gradient Tris-Acetate gels (ThermoFisher Scientific # EA0375) followed by silver staining of the gels using SilverQuest Silver Staining Kit (INVITROGEN, # LC6070) as per manufacturer's instructions.

Lp(a) and LDL internalization assay by flow cytometry

Wild type HuH7 cells and LDLR knockout clonal cells (derived as previously described[25]) were seeded at 20% confluence in 12 well plates 2 days earlier to achieve ~70%-80% confluence on the day of analysis. For uptake assays, cells were washed with serum free DMEM (Dulbecco's Modified Eagle Medium) and then incubated in DMEM containing either 10 µg/ml conjugated

Lp(a) or 4 µg/ml conjugated LDL at 37°C for 2 hours or 1 hour, respectively. For the Lp(a) dose response experiment, cells were subjected to increasing concentrations of labeled Lp(a) ranging from 0.1µg/ml to 40 µg /ml in DMEM. Time course experiment was performed by incubating cells with 10µg/ml of labeled Lp(a) for time periods ranging from 0-24 hrs. Cells were harvested with TrypLE express (ThermoFisher Scientific), washed twice with ice cold PBS, resuspended in 70 µl of ice-cold PBS, and analyzed with a Bio-Rad Ze5 flow cytometer (Everest software, bandpass filter for PE). Data analysis was performed with FlowJo software.

Whole genome CRISPR screen

For each independent biological replicate, a total of ~60 million HuH7 cells were distributed in 10 separate 15 cm2 cell culture plates. Cells were transduced with a pooled library of lentivirus containing the whole genome GeCKOv2 library [23] at an estimated multiplicity of infection of 0.5-1. To select for transduced cells puromycin was added at a final concentration of 2.5 µg/ml the following day and was maintained until selection was complete as determined by the death of uninfected control cells. Cells were passaged every 3 days to maintain logarithmic phase growth with a minimum of ~30 million cells, representing>200X coverage of the library, at all times. On day 14 post-transduction, Lp(a) uptake was assessed. After an initial wash with serum free DMEM, cells were incubated with 20 ug/ml fluorescently labelled Lp(a) in serum free DMEM for 2 hrs at 37°C. Cells were then detached with TrypLE express (ThermoFisher Scientific), collected in ice cold D10, centrifuged at 500g for 5 minutes, washed twice with ice cold FACS buffer (2% FBS in PBS), incubated in 5 uM SYTOX Blue Dead Cell Stain (Fisher, S34857) for 3 minutes, washed again with ice cold FACS buffer, resuspended in 1.5ml cold FACS buffer, and filtered into FACS tube and kept on ice until the time of sorting. Cells were analyzed and sorted with a BD FACSAria III cell sorter (Bandpass filter for fluorophore PE). Subpopulations

of edited cells with the top and bottom 10% of Lp(a) fluorescence were isolated and their genomic DNA was extracted using a DNEasy DNA isolation kit (Qiagen, Hilden, Germany). Amplicon libraries for NextGen sequencing were prepared in two rounds as previously described[23, 41], where in the first round 20 cycle of PCR amplification of integrated gRNA was done followed by addition of NGS barcode in the second round of 11 cycle PCR. Barcoded samples were pooled and sequenced. FASTQ files obtained from NextGen sequencing run were processed by PoolQ to deconvolute the sequencing reads, and individual gRNA and gene-level enrichment analysis in Lp(a) low vs Lp(a) high population was performed using MAGeCK[42]. The top hits with an FDR of 20% were analyzed for predicted and known protein-protein interaction using STRING database. Correlation analysis of the hits from prior genome-wide LDL uptake screen[25] with the results from Lp(a) screen was done by plotting the log2FC values for the modifiers from both screens.

3.5 References

1. Pietiäinen, V., et al., NDRG1 functions in LDL receptor trafficking by regulating endosomal recycling and degradation. J Cell Sci, 2013. 126(Pt 17): p. 3961-71.
2. Spence, J.D. and M. Koschinsky, Mechanisms of lipoprotein(a) pathogenicity: prothrombotic, proatherosclerotic, or both? Arterioscler Thromb Vasc Biol, 2012. 32(7): p. 1550-1.
3. van der Valk, F.M., et al., Oxidized Phospholipids on Lipoprotein(a) Elicit Arterial Wall Inflammation and an Inflammatory Monocyte Response in Humans. Circulation, 2016. 134(8): p. 611-24.
4. Clarke, R., et al., Genetic variants associated with Lp(a) lipoprotein level and coronary disease. N Engl J Med, 2009. 361(26): p. 2518-28.
5. Nikpay, M., et al., A comprehensive 1,000 Genomes-based genome-wide association meta-analysis of coronary artery disease. Nat Genet, 2015. 47(10): p. 1121-1130.
6. Burgess, S., et al., Association of LPA Variants With Risk of Coronary Disease and the Implications for Lipoprotein(a)-Lowering Therapies: A Mendelian Randomization Analysis. JAMA Cardiol, 2018. 3(7): p. 619-627.
7. Thanassoulis, G., et al., Genetic associations with valvular calcification and aortic stenosis. N Engl J Med, 2013. 368(6): p. 503-12.

8. Cairns, B.J., et al., A Replicated, Genome-Wide Significant Association of Aortic Stenosis With a Genetic Variant for Lipoprotein(a): Meta-Analysis of Published and Novel Data. Circulation, 2017. 135(12): p. 1181-1183.
9. Arsenault, B.J., et al., Lipoprotein(a) levels, genotype, and incident aortic valve stenosis: a prospective Mendelian randomization study and replication in a case-control cohort. Circ Cardiovasc Genet, 2014. 7(3): p. 304-10.
10. Becker, L., et al., Identification of a critical lysine residue in apolipoprotein B-100 that mediates noncovalent interaction with apolipoprotein(a). J Biol Chem, 2001. 276(39): p. 36155-62.
11. Cesaro, A., et al., Lipoprotein(a): a genetic marker for cardiovascular disease and target for emerging therapies. J Cardiovasc Med (Hagerstown), 2021. 22(3): p. 151-161.
12. Coassin, S. and F. Kronenberg, Lipoprotein(a) beyond the kringle IV repeat polymorphism: The complexity of genetic variation in the LPA gene. Atherosclerosis, 2022. 349: p. 17-35.
13. White, A.L., B. Guerra, and R.E. Lanford, Influence of allelic variation on apolipoprotein(a) folding in the endoplasmic reticulum. J Biol Chem, 1997. 272(8): p. 5048-55.
14. Schachtl-Riess, J.F., et al., Frequent LPA KIV-2 Variants Lower Lipoprotein(a) Concentrations and Protect Against Coronary Artery Disease. J Am Coll Cardiol, 2021. 78(5): p. 437-449.
15. Coassin, S., et al., A novel but frequent variant in LPA KIV-2 is associated with a pronounced Lp(a) and cardiovascular risk reduction. Eur Heart J, 2017. 38(23): p. 1823-1831.
16. Cain, W.J., et al., Lipoprotein [a] is cleared from the plasma primarily by the liver in a process mediated by apolipoprotein [a]. J Lipid Res, 2005. 46(12): p. 2681-91.
17. Alonso, R., et al., Lipoprotein(a) levels in familial hypercholesterolemia: an important predictor of cardiovascular disease independent of the type of LDL receptor mutation. J Am Coll Cardiol, 2014. 63(19): p. 1982-9.
18. Nestel, P., Lipoprotein(a) Removal Still a Mystery. J Am Heart Assoc, 2019. 8(4): p. e011903.
19. Rader, D.J., et al., The low density lipoprotein receptor is not required for normal catabolism of Lp(a) in humans. J Clin Invest, 1995. 95(3): p. 1403-8.
20. McCormick, S.P.A. and W.J. Schneider, Lipoprotein(a) catabolism: a case of multiple receptors. Pathology, 2019. 51(2): p. 155-164.
21. Clark, J.R., et al., Sortilin enhances secretion of apolipoprotein(a) through effects on apolipoprotein B secretion and promotes uptake of lipoprotein(a). J Lipid Res, 2022. 63(6): p. 100216.
22. Kyle R. Gee, E.A.A., Hee Chol Kang, 4-Sulfotetrafluorophenyl(STP)Esters: NewWater-SolubleAmine-ReactiveReagents for Labeling Biomolecules. 1999.
23. Sanjana, N.E., O. Shalem, and F. Zhang, Improved vectors and genome-wide libraries for CRISPR screening. Nat Methods, 2014. 11(8): p. 783-784.
24. Zhang, L., et al., The IDOL-UBE2D complex mediates sterol-dependent degradation of the LDL receptor. Genes Dev, 2011. 25(12): p. 1262-74.
25. Emmer, B.T., et al., Genome-scale CRISPR screening for modifiers of cellular LDL uptake. PLoS Genet, 2021. 17(1): p. e1009285.

26. Yamauchi, T., et al., Targeted disruption of AdipoR1 and AdipoR2 causes abrogation of adiponectin binding and metabolic actions. Nat Med, 2007. 13(3): p. 332-9.
27. Vuorio, A., et al., Familial hypercholesterolemia and elevated lipoprotein(a): double heritable risk and new therapeutic opportunities. J Intern Med, 2020. 287(1): p. 2-18.
28. Chemello, K., et al., Lipoprotein metabolism in familial hypercholesterolemia. J Lipid Res, 2021. 62: p. 100062.
29. Kraft, H.G., et al., Lipoprotein(a) in homozygous familial hypercholesterolemia. Arterioscler Thromb Vasc Biol, 2000. 20(2): p. 522-8.
30. Durrington, P.N., et al., Lipoprotein (a) in familial hypercholesterolaemia. Curr Opin Lipidol, 2022.
31. Rader, D.J., et al., The inverse association of plasma lipoprotein(a) concentrations with apolipoprotein(a) isoform size is not due to differences in Lp(a) catabolism but to differences in production rate. J Clin Invest, 1994. 93(6): p. 2758-63.
32. de Boer, L.M., et al., Statin therapy and lipoprotein(a) levels: a systematic review and meta-analysis. Eur J Prev Cardiol, 2022. 29(5): p. 779-792.
33. Lambert, G., et al., The complexity of lipoprotein (a) lowering by PCSK9 monoclonal antibodies. Clin Sci (Lond), 2017. 131(4): p. 261-268.
34. Alonso, R., et al., PCSK9 and lipoprotein (a) levels are two predictors of coronary artery calcification in asymptomatic patients with familial hypercholesterolemia. Atherosclerosis, 2016. 254: p. 249-253.
35. Mayne, J., et al., Plasma PCSK9 levels are significantly modified by statins and fibrates in humans. Lipids Health Dis, 2008. 7: p. 22.
36. Croyal, M., et al., PCSK9 inhibition with alirocumab reduces lipoprotein(a) levels in nonhuman primates by lowering apolipoprotein(a) production rate. Clin Sci (Lond), 2018. 132(10): p. 1075-1083.
37. Yang, X.P., et al., Scavenger receptor-BI is a receptor for lipoprotein(a). J Lipid Res, 2013. 54(9): p. 2450-7.
38. Sharma, M., et al., Recycling of Apolipoprotein(a) After PlgRKT-Mediated Endocytosis of Lipoprotein(a). Circ Res, 2017. 120(7): p. 1091-1102.
39. Romagnuolo, R., et al., Lipoprotein(a) catabolism is regulated by proprotein convertase subtilisin/kexin type 9 through the low density lipoprotein receptor. J Biol Chem, 2015. 290(18): p. 11649-62.
40. Romagnuolo, R., et al., Roles of the low density lipoprotein receptor and related receptors in inhibition of lipoprotein(a) internalization by proprotein convertase subtilisin/kexin type 9. PLoS One, 2017. 12(7): p. e0180869.
41. Shalem, O., et al., Genome-scale CRISPR-Cas9 knockout screening in human cells. Science, 2014. 343(6166): p. 84-87.
42. Li, W., et al., MAGeCK enables robust identification of essential genes from genome-scale CRISPR/Cas9 knockout screens. Genome Biol, 2014. 15(12): p. 554.

Chapter 4 Conclusion and Future Directions

Receptor-mediated endocytosis is an important process by which many macromolecules enter eukaryotic cells[1]. This process is initiated with the binding of a ligand to a specific receptor spanning the plasma membrane and its internalization into endocytic vesicles[2]. The endosomal acidic environment may induce conformational change in the receptor causing receptor-ligand complex dissociation, after which the receptor may recycle back to the plasma membrane[3].

The level of LDL in the circulation is maintained by a balance of new LDL generation and receptor mediated clearance, with reduction in the latter process leading to hypercholesterolemia and cardiovascular diseases[4, 5]. Chapter 1 provides background on the molecular pathways that are known to govern LDL homeostasis, including the expression and trafficking of the LDL receptor (LDLR). LDLR is a plasma membrane protein that is expressed predominantly on hepatocytes and continually recycles to the cell surface after endocytosis and release of LDL. Although several studies have identified the molecular determinants of LDLR endocytosis, our understanding of LDLR recycling has remained limited. The work described in chapter 2 establishes a previously unrecognized role for a small GTPase, RAB10, in the trafficking of internalized LDLR from the endocytic recycling compartment to the cell surface. We show that RAB10 not only facilitates the recycling of LDLR but also that of the transferrin receptor (TFR), a protein involved in the regulation of cellular iron stores. RAB10 promotes trafficking of these two receptors from different endosomal compartments to the cell surface.

However, the exact mechanism by which RAB10 facilitates trafficking of LDLR and TFR carrying vesicles from different compartments remains unclear. Our prior genome-wide CRISPR screen similarly identified multiple components of the exocyst complex (EXOC1, EXOC2, EXOC3, EXOC4, EXOC7, and EXOC8), with a similar functional influence on LDL and transferrin uptake as RAB10, suggesting that they may function in the same pathway. The exocyst complex has previously been shown to interact with RAB10 and other RAB GTPases to regulate vesicle trafficking[6, 7]. It is therefore plausible that the impact of RAB10 on LDLR and TFR involves the recruitment of these components. Other modifiers including RABIF (Rab interacting factor), known to stimulate GDP release from RAB10, and STX4, a SNARE protein that facilitates docking and fusion of transport vesicle were also identified in the screen and were previously shown to associate with RAB GTPases [8-10], suggesting that RAB10 may promote vesicle recycling by recruiting and interacting with these proteins and thereby coordinate the formation, trafficking, tethering, and fusion of LDLR and TFR-containing vesicles. Future studies should investigate the plausible coordination of RAB10 with these proteins for transport of vesicles carrying LDL and TFR receptors.

Our results are based on in vitro studies, and future work could address the physiologic relevance of RAB10 on LDLR and TFR trafficking in vivo. Germline deletion of RAB10 in mice causes embryonic lethality[11], which also suggests a broad cellular function for RAB10, consistent with previous studies demonstrating the role of RAB10 in multiple trafficking pathways involving various intracellular compartments [6, 12, 13]. However, future studies could address hepatic RAB10 function in LDL homeostasis in vivo through the generation and phenotypic characterization of a conditional knockout mouse model. Our results, together with previous findings, support a global role for RAB10 in vesicle trafficking and suggest that

multiple cargoes may depend on RAB10 for trafficking. This broad role of RAB10 could limit the potential for developing RAB10 targeted therapeutic for enhancing LDL uptake.

Elevated levels of Lp(a) also lead to the development and progression of atherosclerosis[14]. As discussed in chapter 1, however, our understanding of the molecular factors that influence Lp(a) levels is very limited, especially in comparison to LDL. This lack of understanding has provided a major barrier to the development of therapeutic approaches for Lp(a)-lowering. In particular, the specific receptor(s) that mediate Lp(a) clearance has not been established[15]. The work reported in chapter 3 describes the first application of a high throughput CRISPR screening approach to interrogate all protein coding genes for their influence on Lp(a) uptake. This screen clearly identified LDLR and several well-established regulators of LDLR, including SCAP and MBTPS2, as positive regulators and MYLIP as a negative regulator of Lp(a) uptake. A similar functional effect was not detected for any other membrane proteins, including several previously proposed receptors. Our results suggest that LDLR is the primary mediator of Lp(a) uptake in HuH7 cells. However, our data do not exclude the possibility of a role for other hypothesized receptors due to several caveats related to genome wide CRISPR screens. For example, genes that are essential for cell survival may not be identified in a CRISPR knockout screen, as the edited cells will be depleted from the population. In addition to essential genes, receptors with redundant function on Lp(a) uptake may also go undetected in a screen as the loss of activity for one gene may be compensated by the other. Inadequate depth of coverage is another major caveat associated with a genome wide screen. Future work will likely apply a secondary screen with a custom library targeting fewer genes with more gRNAs per gene, in order to improve the power of detection for validation and refinement of the candidates identified in the primary screen. Although our finding suggests that LDLR may function as a key clearance

receptor for Lp(a), future work could more fully characterize the interaction between Lp(a) and LDLR, including dissecting the involvement of specific Lp(a) protein components as well as the specific domains that mediate interaction with LDLR.

Altogether our screen hits provide additional support for previously studied role of LDLR as a mediator for Lp(a) uptake, suggesting LDLR regulation as a potential therapeutic target for lowering Lp(a) level. LDLR expression is regulated by the SREBP2 pathway. However, data on statins, a class of drugs that upregulate hepatic LDLR expression through activation of the SREBP2 pathway, showed mixed results on Lp(a) level in patients[16-18]. On the other hand, targeting PCSK9, a negative regulator of LDLR, has been shown to reduce Lp(a) level by an unclear mechanism, where some studies indicate that PCSK9 inhibitors increase LDLR-mediated uptake of Lp(a)[19, 20], while other study showed that PCSK9 inhibitor reduces synthesis and secretion of Lp(a)[21]. Statins also increase PCSK9 expression through activation of the SREBP2 pathway. It is therefore possible that the impact of statins on Lp(a) is attenuated due to upregulation of PCSK9. A recent study showed that Lp(a) catabolism is increased in patients receiving combined treatment with statin and PCSK9 inhibitor[19]. Statin may also increase Lp(a) expression as shown by study where cells treated with statins had increased expression of *LPA* mRNA and apolipoprotein(a) protein[22]. Future studies are required to address the mechanism underlying the ineffectiveness of statins on Lp(a) level. Comparison of Lp(a) uptake in statin treated wild type cells, PCSK9 knockout cells, and LDLR knockout cells would validate whether the effect of statin on invitro Lp(a) uptake is due to PCSK9 or other unknown mechanism. IDOL, encoded by MYLIP gene, which was also enriched in our screen, might be another potential therapeutic target for lowering Lp(a). IDOL is a negative regulator of LDLR and unlike LDLR and PCSK9, IDOL is not regulated by the SREBP2 pathway[23]. Therefore,

pharmacologic inhibition of IDOL could increase LDLR level without increasing PCSK9 and as a result increase Lp(a) uptake.

4.1 References

1. Gao, H., W. Shi, and L.B. Freund, Mechanics of receptor-mediated endocytosis. Proc Natl Acad Sci U S A, 2005. 102(27): p. 9469-74.
2. Grant, B.D. and J.G. Donaldson, Pathways and mechanisms of endocytic recycling. Nat Rev Mol Cell Biol, 2009. 10(9): p. 597-608.
3. Maxfield, F.R. and T.E. McGraw, Endocytic recycling. Nat Rev Mol Cell Biol, 2004. 5(2): p. 121-32.
4. Vos, D., J.A. Kuivenhoven, and B. van de Sluis, Recycling the LDL receptor to combat atherosclerosis. Aging (Albany NY), 2018. 10(12): p. 3638-3640.
5. Yang, H.X., et al., Cholesterol in LDL receptor recycling and degradation. Clin Chim Acta, 2020. 500: p. 81-86.
6. Babbey, C.M., R.L. Bacallao, and K.W. Dunn, Rab10 associates with primary cilia and the exocyst complex in renal epithelial cells. Am J Physiol Renal Physiol, 2010. 299(3): p. F495-506.
7. Sano, H., et al., A potential link between insulin signaling and GLUT4 translocation: Association of Rab10-GTP with the exocyst subunit Exoc6/6b. Biochem Biophys Res Commun, 2015. 465(3): p. 601-5.
8. Gulbranson, D.R., et al., RABIF/MSS4 is a Rab-stabilizing holdase chaperone required for GLUT4 exocytosis. Proc Natl Acad Sci U S A, 2017. 114(39): p. E8224-e8233.
9. Clague, M.J. and S. Urbé, Data mining for traffic information. Traffic, 2020. 21(1): p. 162-168.
10. Wilcke, M., et al., Rab11 regulates the compartmentalization of early endosomes required for efficient transport from early endosomes to the trans-golgi network. J Cell Biol, 2000. 151(6): p. 1207-20.
11. Lv, P., et al., Targeted disruption of Rab10 causes early embryonic lethality. Protein Cell, 2015. 6(6): p. 463-467.
12. Babbey, C.M., et al., Rab10 regulates membrane transport through early endosomes of polarized Madin-Darby Canine Kidney cells. Molecular Biology of the Cell, 2006. 17(7): p. 3156-3175.
13. Chua, C.E.L. and B.L. Tang, Rab 10-a traffic controller in multiple cellular pathways and locations. J Cell Physiol, 2018. 233(9): p. 6483-6494.
14. Cesaro, A., et al., Lipoprotein(a): a genetic marker for cardiovascular disease and target for emerging therapies. J Cardiovasc Med (Hagerstown), 2021. 22(3): p. 151-161.
15. McCormick, S.P.A. and W.J. Schneider, Lipoprotein(a) catabolism: a case of multiple receptors. Pathology, 2019. 51(2): p. 155-164.
16. de Boer, L.M., et al., Statin therapy and lipoprotein(a) levels: a systematic review and meta-analysis. Eur J Prev Cardiol, 2022. 29(5): p. 779-792.

17. Watts, G.F., et al., Controlled study of the effect of proprotein convertase subtilisin-kexin type 9 inhibition with evolocumab on lipoprotein(a) particle kinetics. Eur Heart J, 2018. 39(27): p. 2577-2585.
18. van Wissen, S., et al., Long term statin treatment reduces lipoprotein(a) concentrations in heterozygous familial hypercholesterolaemia. Heart, 2003. 89(8): p. 893-6.
19. Watts, G.F., et al., PCSK9 Inhibition with alirocumab increases the catabolism of lipoprotein(a) particles in statin-treated patients with elevated lipoprotein(a). Metabolism, 2020. 107: p. 154221.
20. Romagnuolo, R., et al., Roles of the low density lipoprotein receptor and related receptors in inhibition of lipoprotein(a) internalization by proprotein convertase subtilisin/kexin type 9. PLoS One, 2017. 12(7): p. e0180869.
21. Villard, E.F., et al., PCSK9 Modulates the Secretion But Not the Cellular Uptake of Lipoprotein(a) Ex Vivo: An Effect Blunted by Alirocumab. JACC Basic Transl Sci, 2016. 1(6): p. 419-427.
22. Tsimikas, S., et al., Statin therapy increases lipoprotein(a) levels. Eur Heart J, 2020. 41(24): p. 2275-2284.
23. Zhang, C.P., et al., IDOL, inducible degrader of low-density lipoprotein receptor, serves as a potential therapeutic target for dyslipidemia. Med Hypotheses, 2016. 86: p. 138-42.